Electronic Supplementary Material (ESI) for New Journal of Chemistry.

Supporting Information for

Killing Two Birds with One Stone: Phosphorylation by a Tabun Mimic and Subsequent Capture of Cyanide Using a Single Fluorescent Chemodosimeter

Rashid Mia[a], Peter J. Cragg[b], Frank R. Fronczek[C] and Karl J. Wallace[a]*

a) Department of Chemistry and Biochemistry, University of Southern Mississippi, Hattiesburg, Mississippi 39406, USA.

b) School of Applied Sciences, University of Brighton, Brighton, BN2 4GJ, UK

c) Department of Chemistry, Louisiana State University, Baton Rouge, Louisiana, 70803, USA

Table of contents **Page Nº**

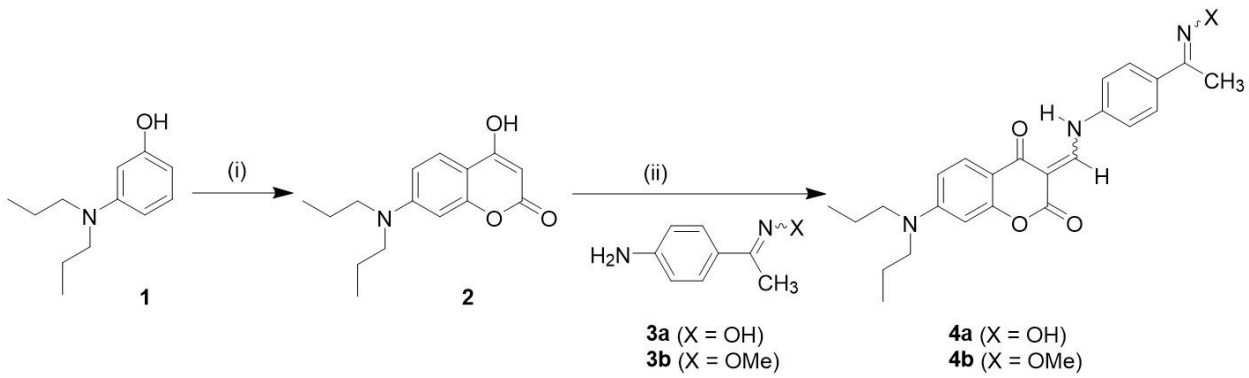

Scheme S1: Synthetic route of **4a** and **4b**; (i) magic malonate, toluene, heated under reflux (ii) triethyl orthoformate, iso-propanol, heated under reflux.

1. 1D and 2D NMR spectra for 4a

Table S1. ^{1}H and ^{13}C NMR assignment for **4a** in DMSO-d_6 at 298 K.

	^{1}H NMR (ppm, *J* = Hz)	**^{1}H NMR (ppm, *J* = Hz)**	**^{13}C NMR (ppm)**	**^{13}C NMR (ppm)**
	E	*Z*	*E*	*Z*
2	NA	NA	162.9	164.0
3	NA	NA	97.5	97.8
4	NA	NA	179.5	176.0
4a	NA	NA	153.1	153.0
5	7.7 (m)	7.7 (m)	127.3	127.3
6	6.63 to 6.65 (m)	6.63 to 6.65 (m)	108.6	108.6
7	NA	NA	107.8	108.1
8	6.35 (*d*, *J* = 2.35)	6.39 (*d*, *J* = 2.35)	96.5	96.6
8a	NA	NA	156.5	156.3
9	8.75 (*d*, *J* = 13.4)	8.80 (*d*, *J* = 14.5)	153.3	151.8
10	NA	NA	138.2	138.7
11/11’	7.56 to 7.55 (*d*, *J* = 8.95)	7.56 to 7.55 (*d*, *J* = 8.95)	118.3	118.8
12/12’	7.7 (m)	7.7 (m)	126.8	126.9
13	NA	NA	134.8	134.8
14	NA	NA	152.1	152.1
15	2.15 (s)	2.15 (s)	11.3	11.3
16	3.30 (m)*	3.30 (m)*	51.9	51.9
17	1.56 (*h*, *J* = 7.41, 7.41, 7.48, 7.48, 7.48)	1.56 (*h*, *J* = 7.41, 7.41, 7.48, 7.48, 7.48)	19.9	19.9
18	0.90 (*t*, *J* = 7.41, 7.41)	0.90 (*t*, *J* = 7.41, 7.41)	11.0	11.0
NH	13.5 (d, *J* = 13.5)	11.57 (*d*, *J* = 14.5)	NA	NA
OH(oxime)	11.2 (*s*)	11.2 (*s*)	NA	NA

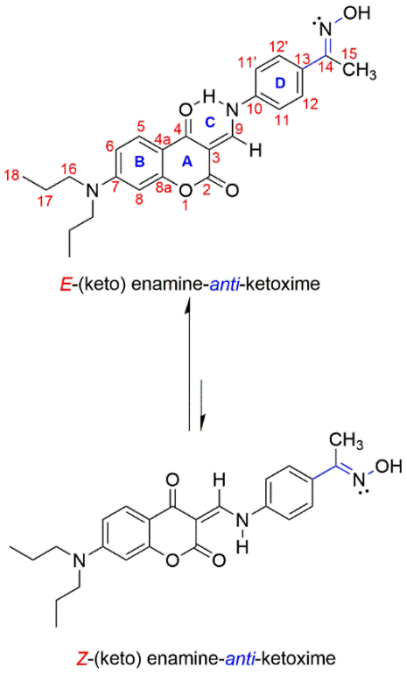

* Signal partially obscured by DMSO

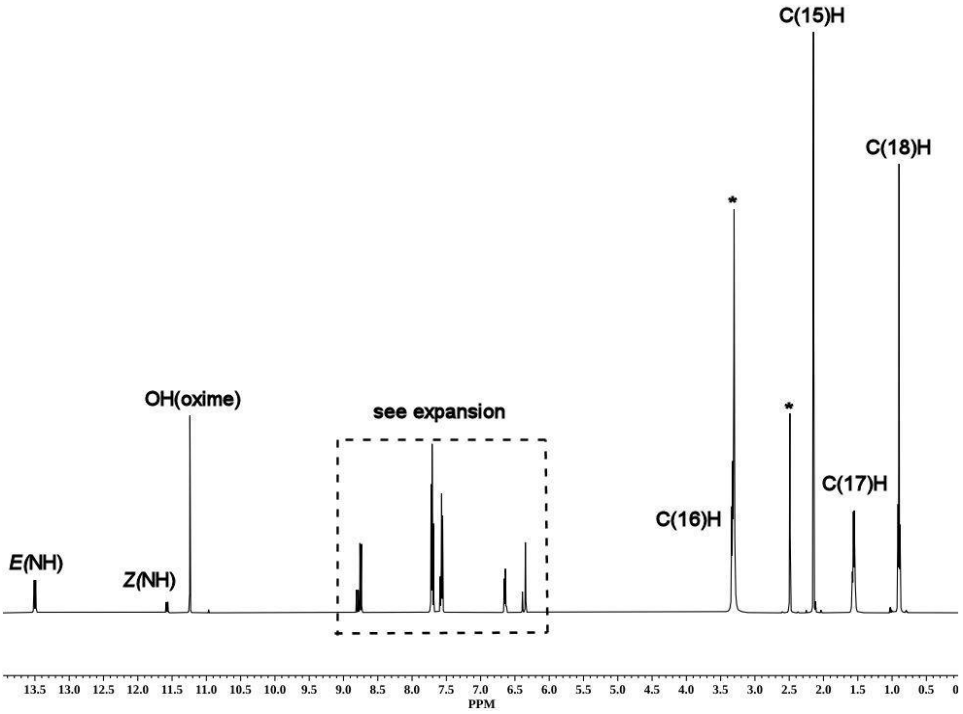

Figure S1. ^{1}H-NMR spectrum of **4a** in DMSO-d_6 at 298 K.

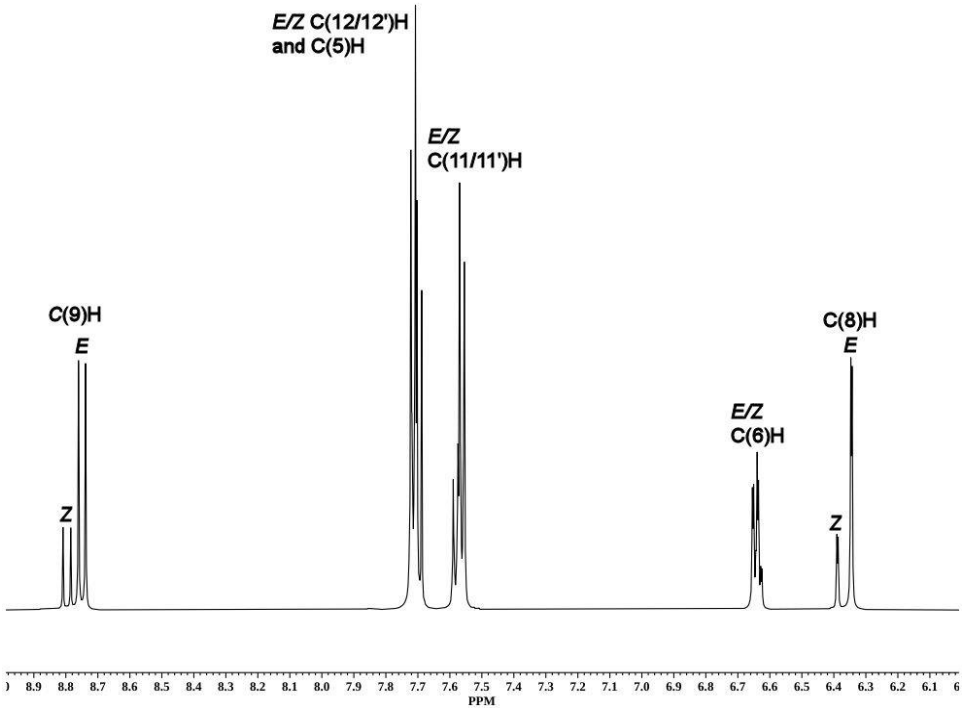

Figure S2. ^{1}H-NMR spectrum (expansion-aromatic region) of **4a** in DMSO-d_6 at 298 K.

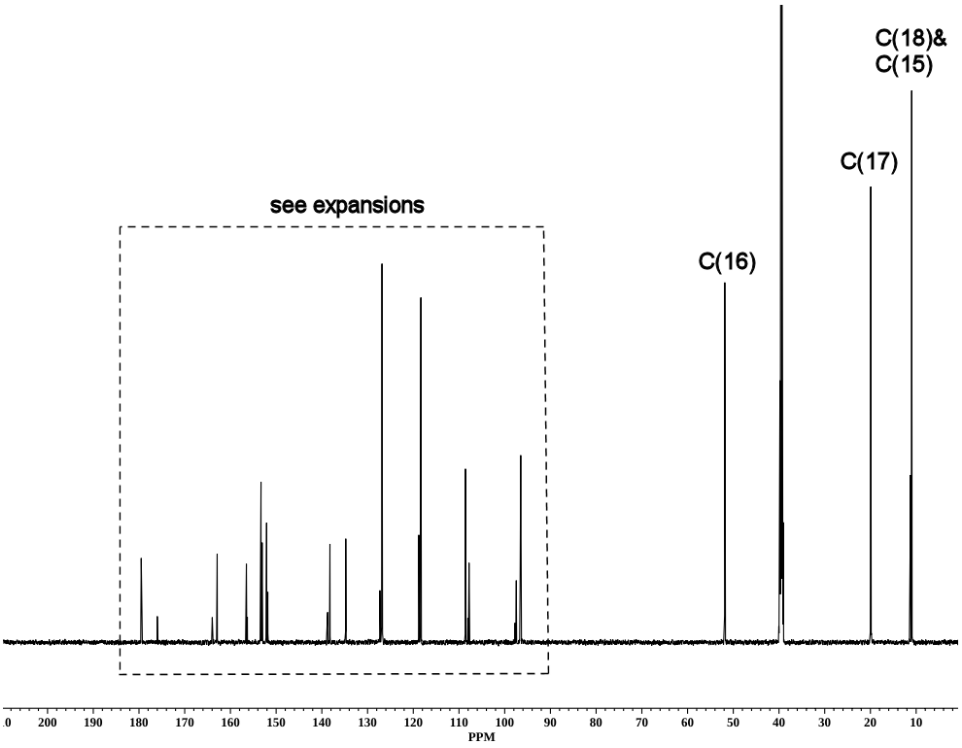

Figure S3. ^{13}C-NMR spectrum of **4a** in DMSO-d_6 at 298 K.

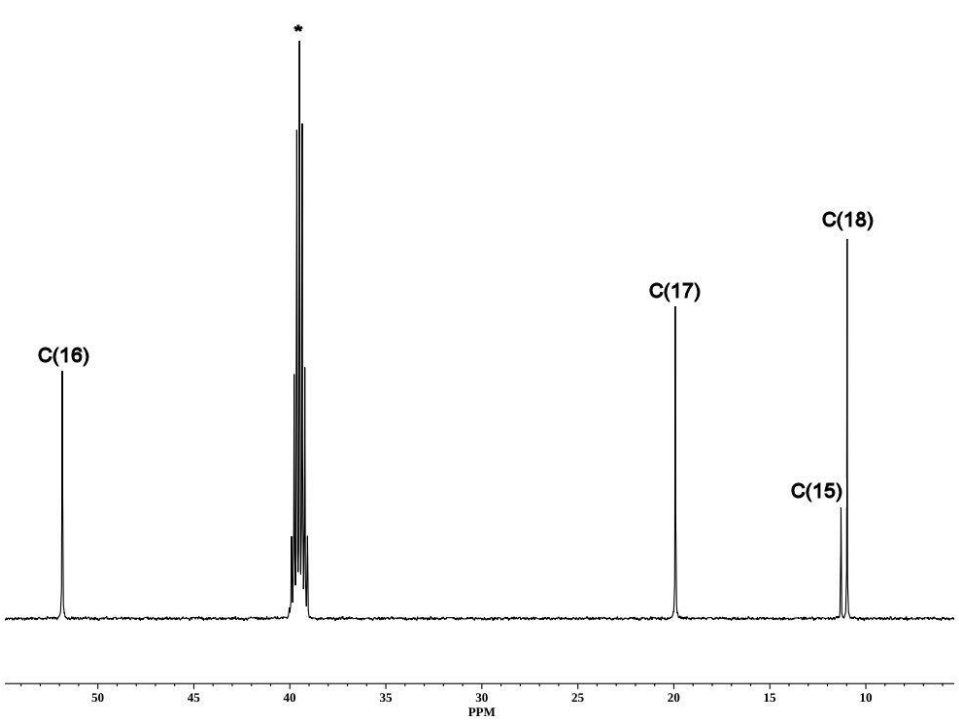

Figure S4. ^{13}C-NMR spectrum (expansion 5 to 55 ppm) of **4a** in DMSO-d_6 at 298 K.

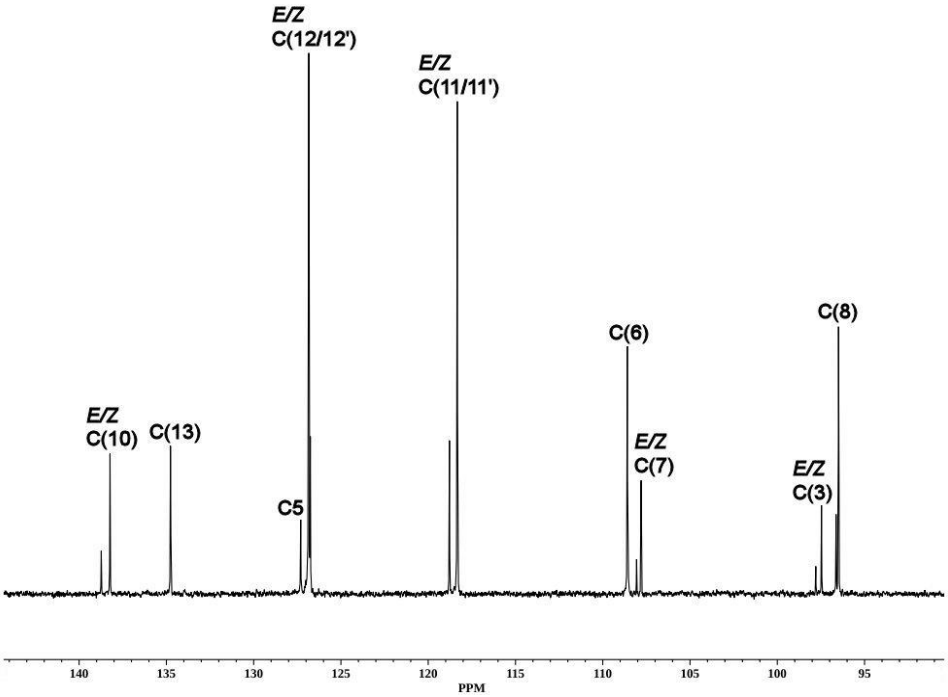

Figure S5. ^{13}C-NMR spectrum (expansion 90 to 145 ppm) of **4a** in DMSO-d_6 at 298 K.

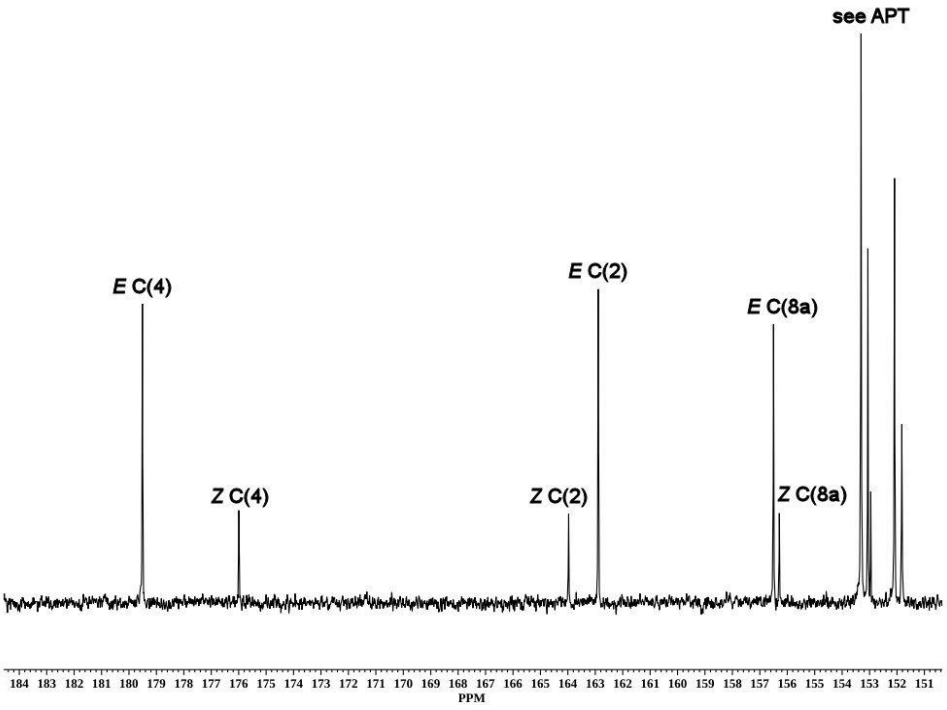

Figure S6. ^{13}C-NMR spectrum (expansion 150 to 185 ppm) of **4a** in DMSO-d_6 at 298 K.

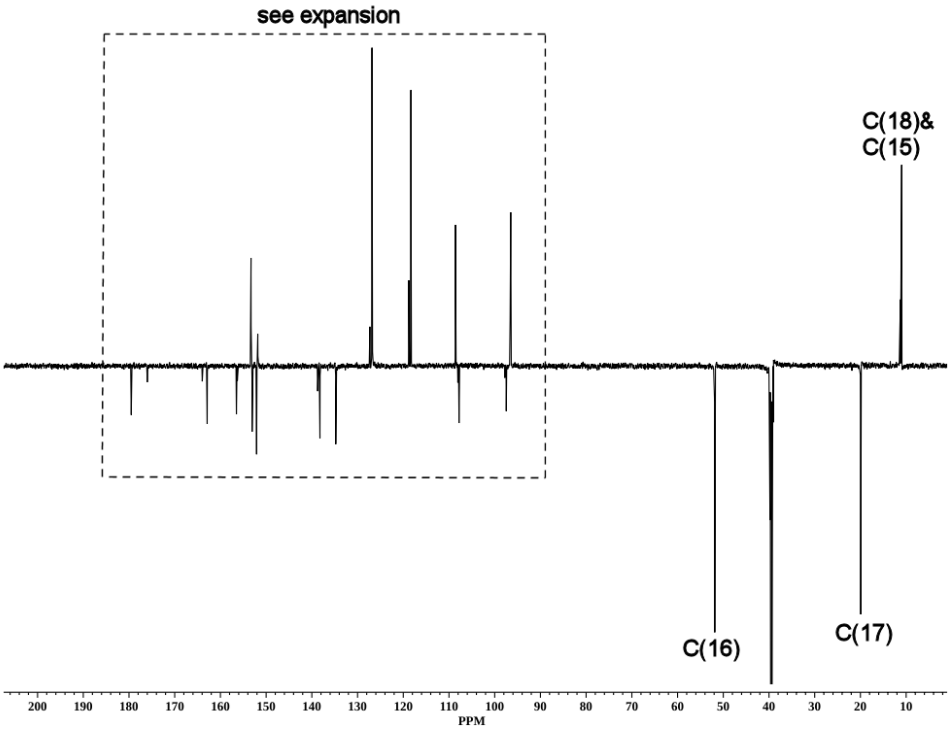

Figure S7. ^{13}C-APT NMR spectrum of **4a** in DMSO-d_6 at 298 K.

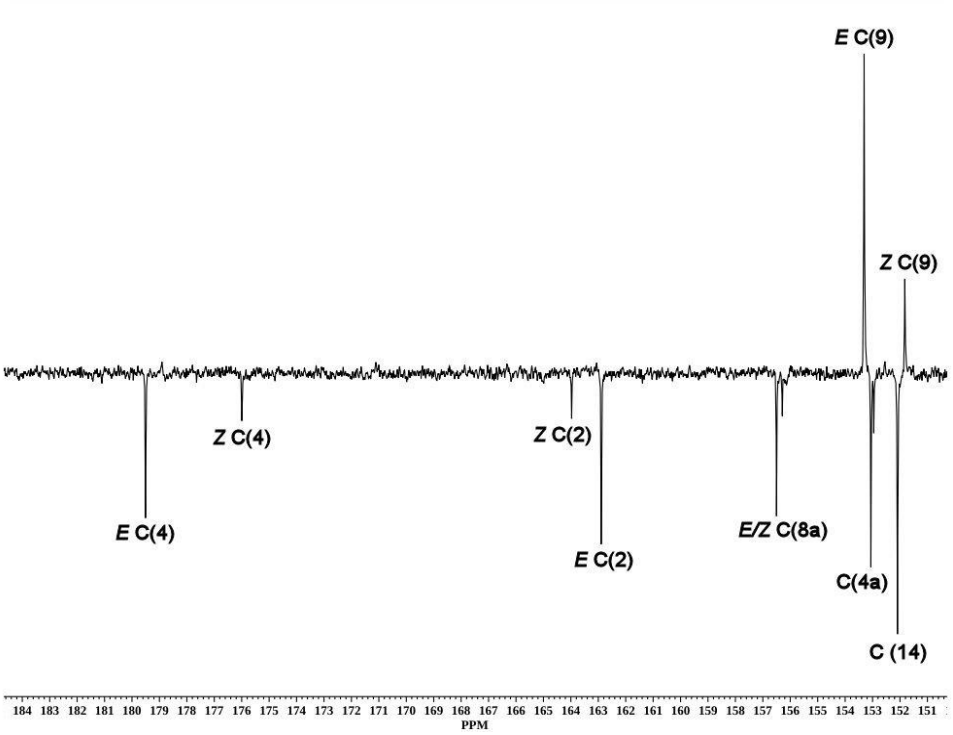

Figure S8. ^{13}C-APT NMR spectrum (expansion 150 to 185 ppm) of **4a** in DMSO-d_6 at 298 K.

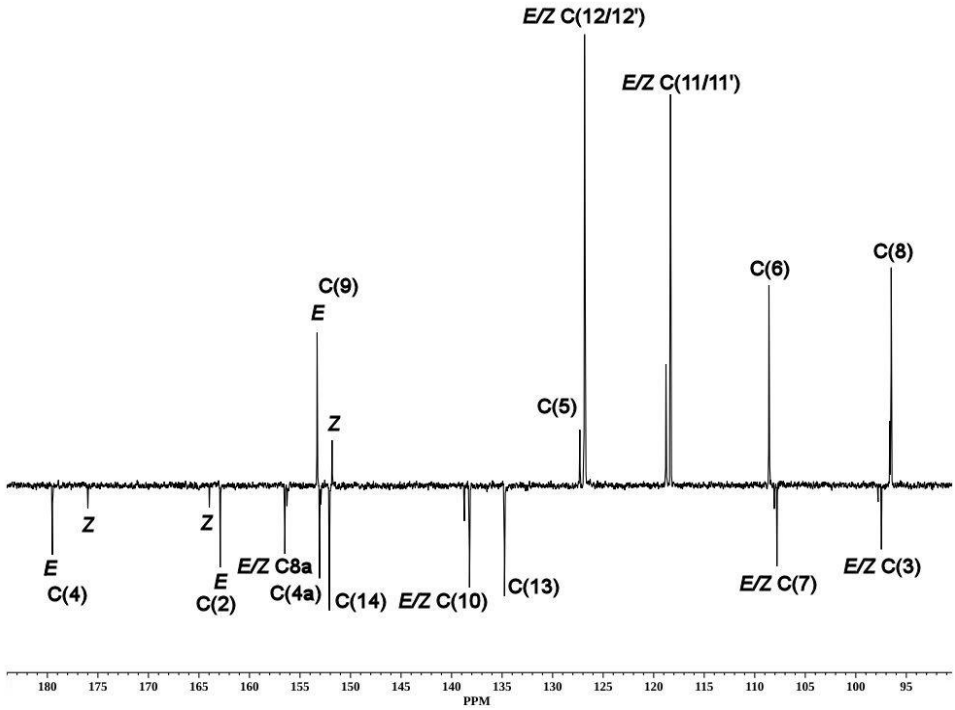

Figure S9. ^{13}C-APT NMR spectrum (expansion 90 to 185 ppm) of **4a** in DMSO-d_6 at 298 K.

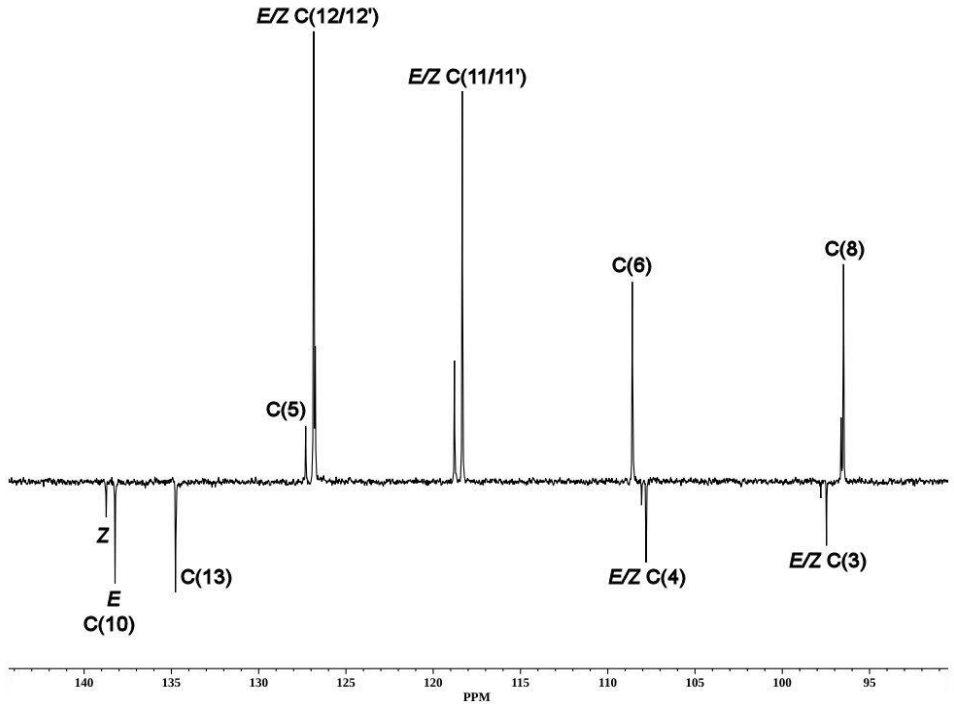

Figure S10. ^{13}C-APT NMR spectrum (expansion 90 to 145 ppm) of **4a** in DMSO-d_6 at 298 K.

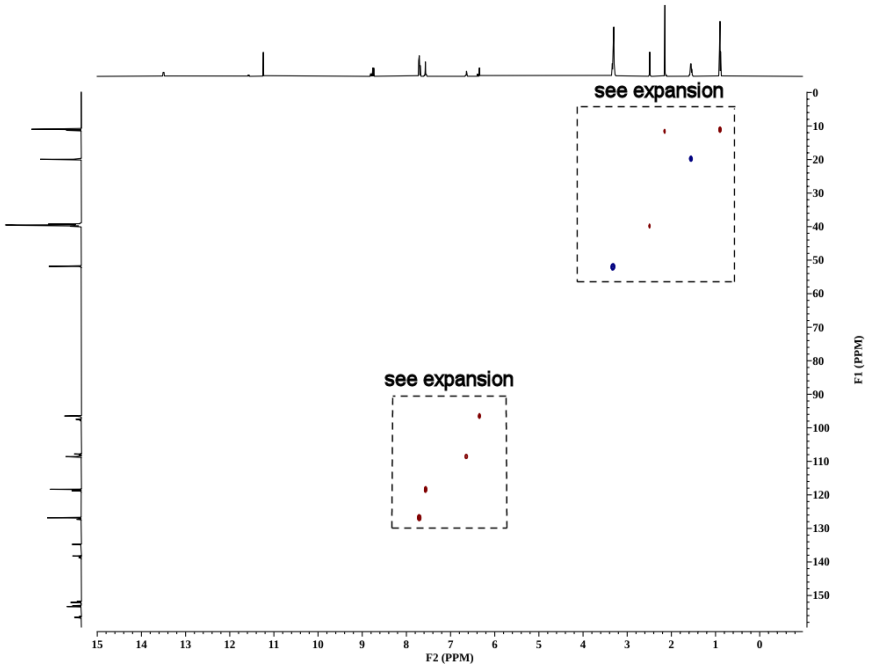

Figure S11. HSQC spectrum of **4a** in DMSO-d_6 at 298 K.

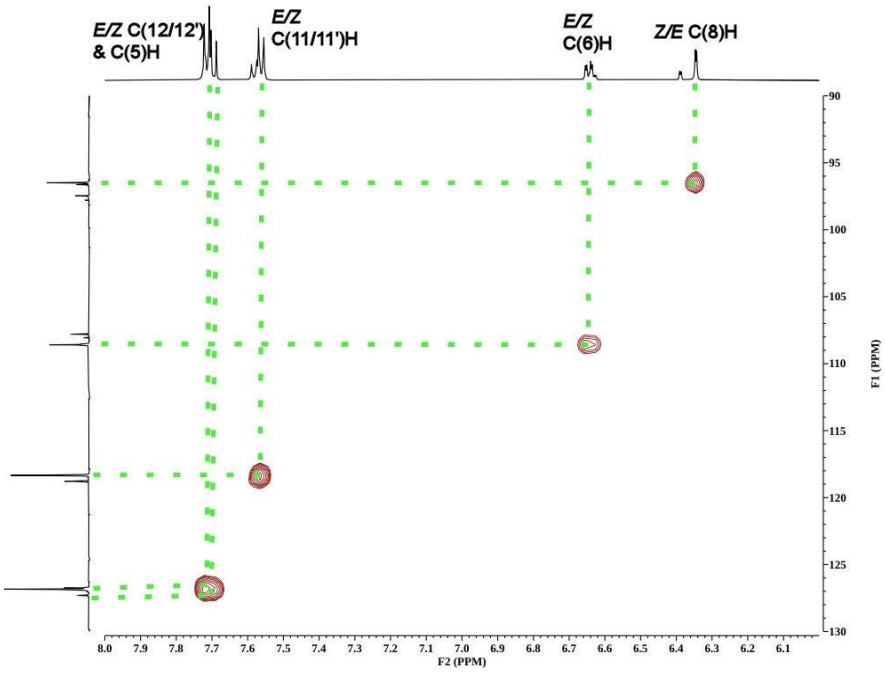

Figure S12. HSQC spectrum (expansion aromatic region) of **4a** in DMSO-d_6 at 298 K.

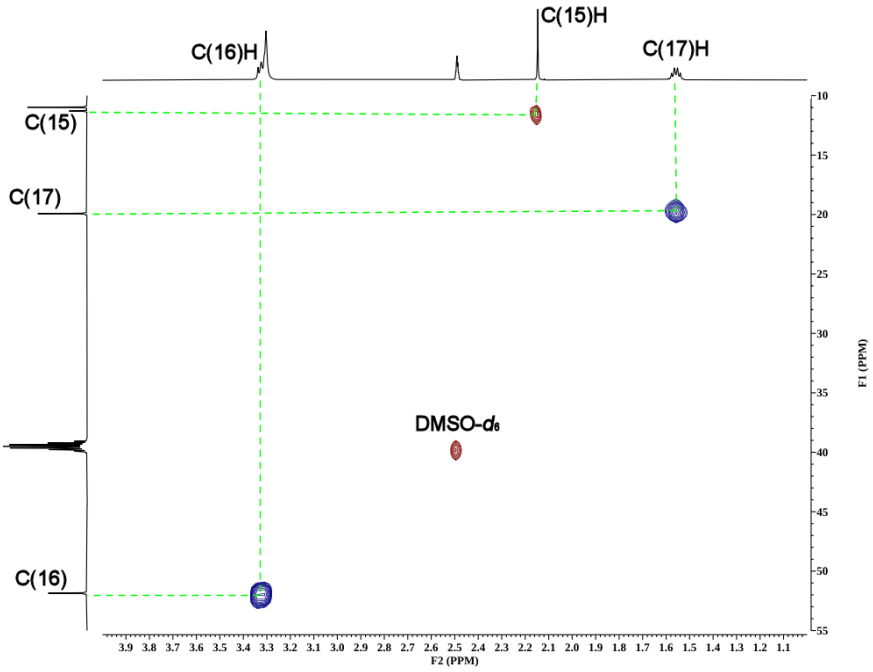

Figure S13. HSQC spectrum (expansion 0.5 to 4.0 ppm) of **4a** in DMSO-d_6 at 298 K.

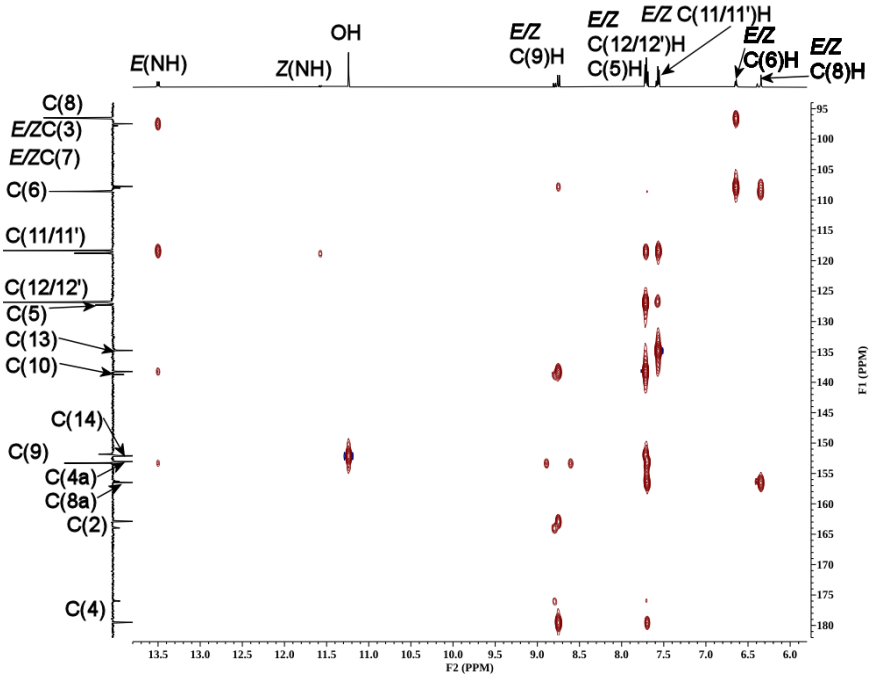

Figure S14. HMBC spectrum (expansion aromatic) of **4a** in DMSO-d_6 at 298 K.

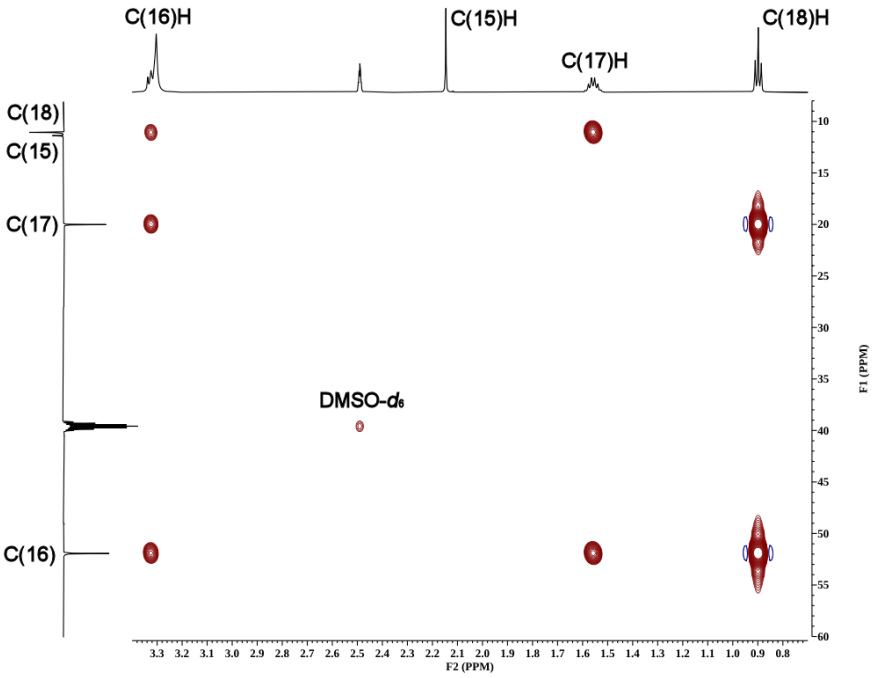

Figure S15. HMBC spectrum (expansion 0.5 to 3.5 ppm) of **4a** in DMSO-d_6 at 298 K.

2. X-ray crystallography structure and packing

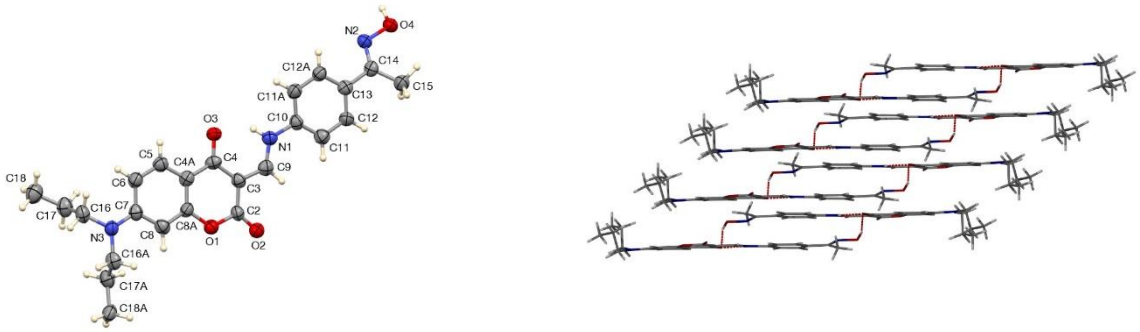

Figure S16. (Left) The molecular structure of **4a**, showing displacement ellipsoids at the 50% probability level, (right) crystal packing.

Table S2. Fluorescence lifetimes (τ) of four tautomer's of **4a** data collected at 298 K.

4a		τ_1(ns) (3σ)	τ_2(ns) (3σ)	$\bar{\tau}$(ns) (3σ)	A (3σ)	χ^2	Norm. pre-exponential	
Em 530 nm	Run (1)	0.79(8)	1.57(2)	1.54(8)	2.6 (5)	1.16	0.03	0.97
	Run (2)	0.82(5)	1.56(3)	1.53(6)	2.5(4)	1.20	0.04	0.96
	Avg.	**0.81(7)**	**1.57(3)**	**1.54(7)**	**1.6(5)**	**1.18**	**0.04**	**0.96**
Em 590 nm	Run (1)	0.23(3)	1.54(2)	1.07(3)	1.3(5)	1.13	0.36	0.64
	Run (1)	0.27(4)	1.55(4)	1.09(4)	1.0(5)	1.12	0.36	0.64
	Avg.	**0.25(4)**	**1.6(2)**	**1.08(4)**	**1.2 (5)**	**1.13**	**0.36**	**0.64**

3. UV-Vis and Fluorescence spectroscopy of 4a, 4a-oximate and adducts and model systems

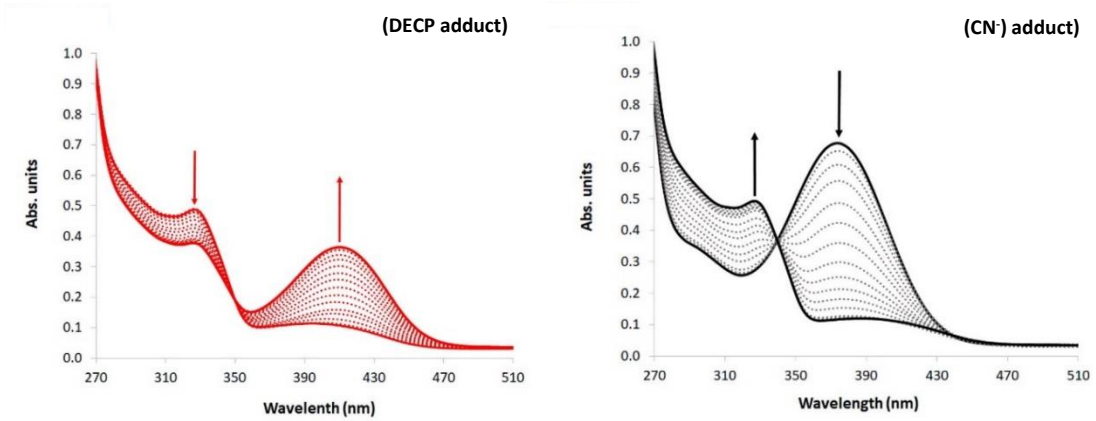

Figure S17. UV-vis titration of **4a**-ketoximate (16 μmol·dm^{-3}, DMSO, 298 K) upon the addition of DECP. The deconvoluted spectra show the phosphorylated adduct (left) and the CN^- adduct (right).

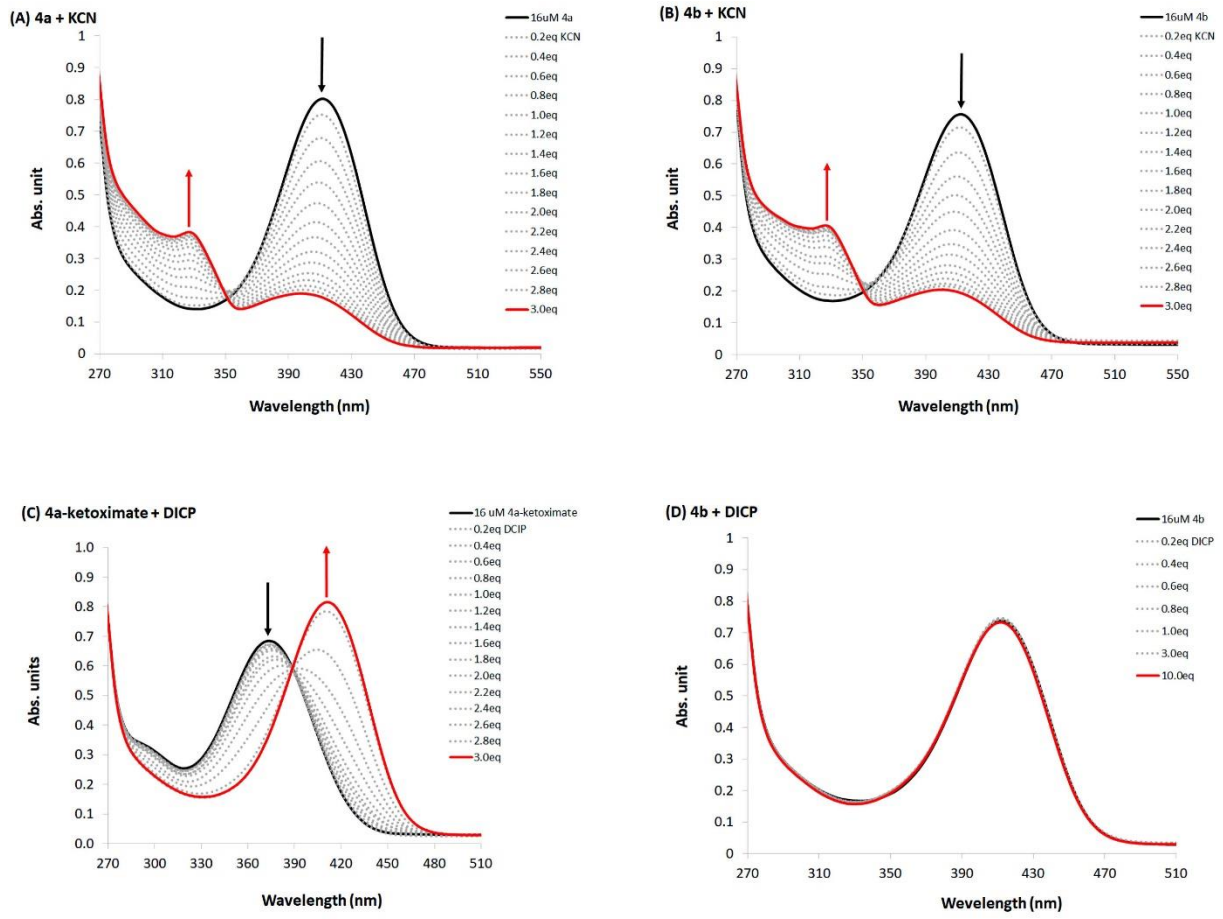

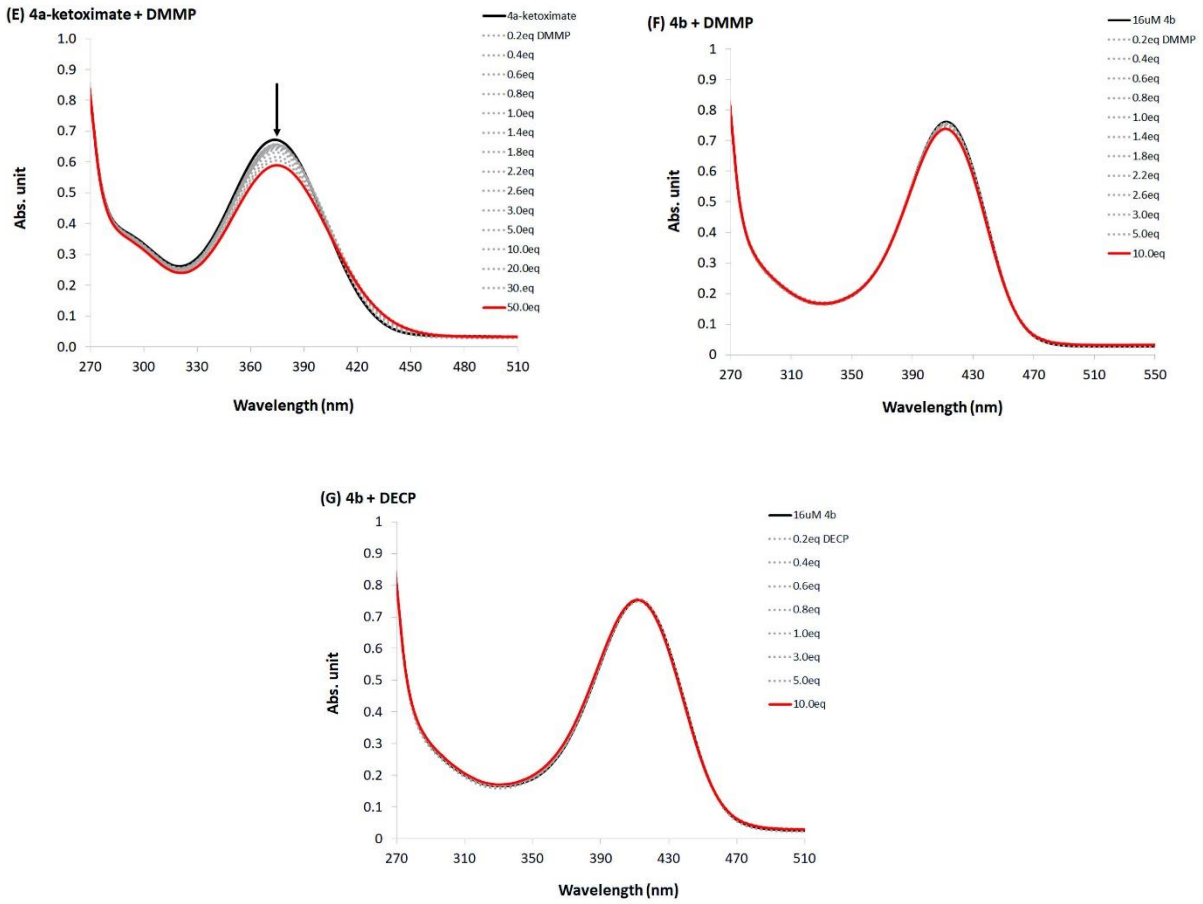

Figure S18. UV-Vis titration spectra of **4a** and model compound **4b** (16 μmol·dm^{-3}, DMSO, 298 K): addition of KCN to **4a** (A) and **4b** (B); addition of aliquots of DICP to **4a** ketoximate (C) and **4b** (D), addition of DMMP to **4a** ketoximate (E) and **4b** (F) and addition of DECP to **4b** (G).

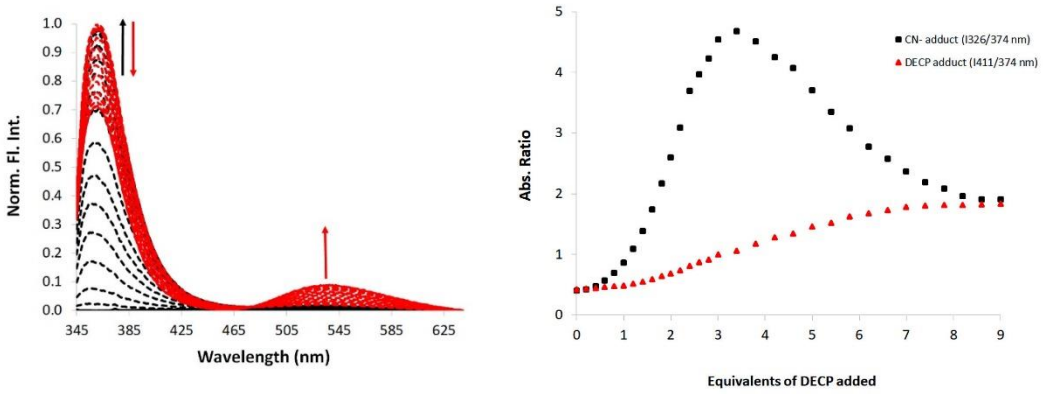

Figure S19. Left, Fluorescence titration of **4a**-ketoximate (16 μmol·dm^{-3}, DMSO, 298 K) upon the addition of aliquots of DECP; Right, binding isotherm.

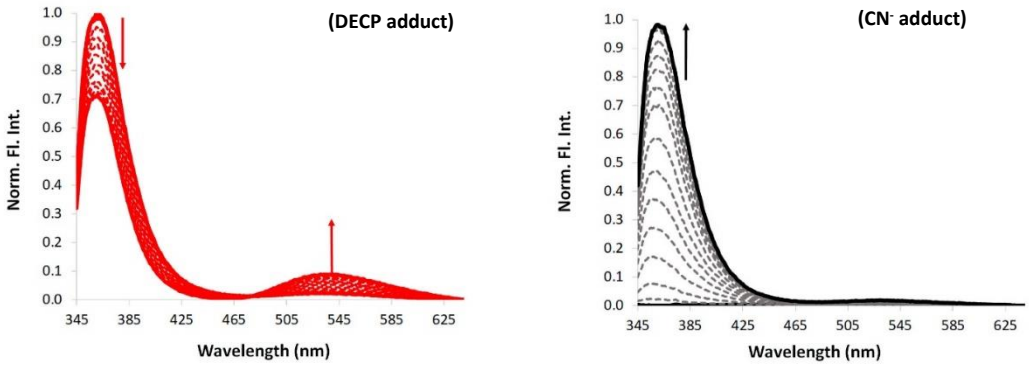

Figure S20. Fluorescence titration of **4a**-ketoximate (16 μmol·dm^{-3}, DMSO, 298 K) upon the addition of DECP showing the two different species –phosphorylation adduct (left) and CN^- adduct (right).

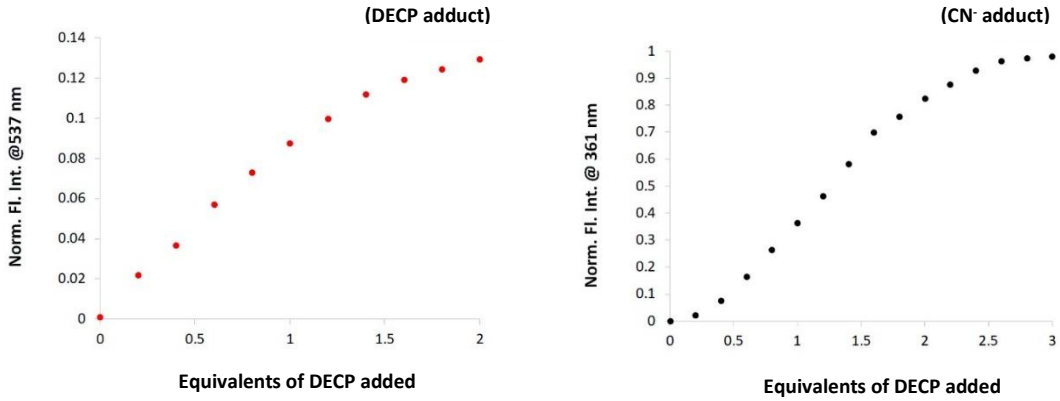

Figure S21. Fluorescence binding isotherms of **4a**-ketoximate (16 μmol·dm^{-3}, DMSO, 298 K) upon the addition of aliquots of DECP lower concentration range 0-3 equivalents. Phosphorylation adduct (left) and CN^- adduct (right).

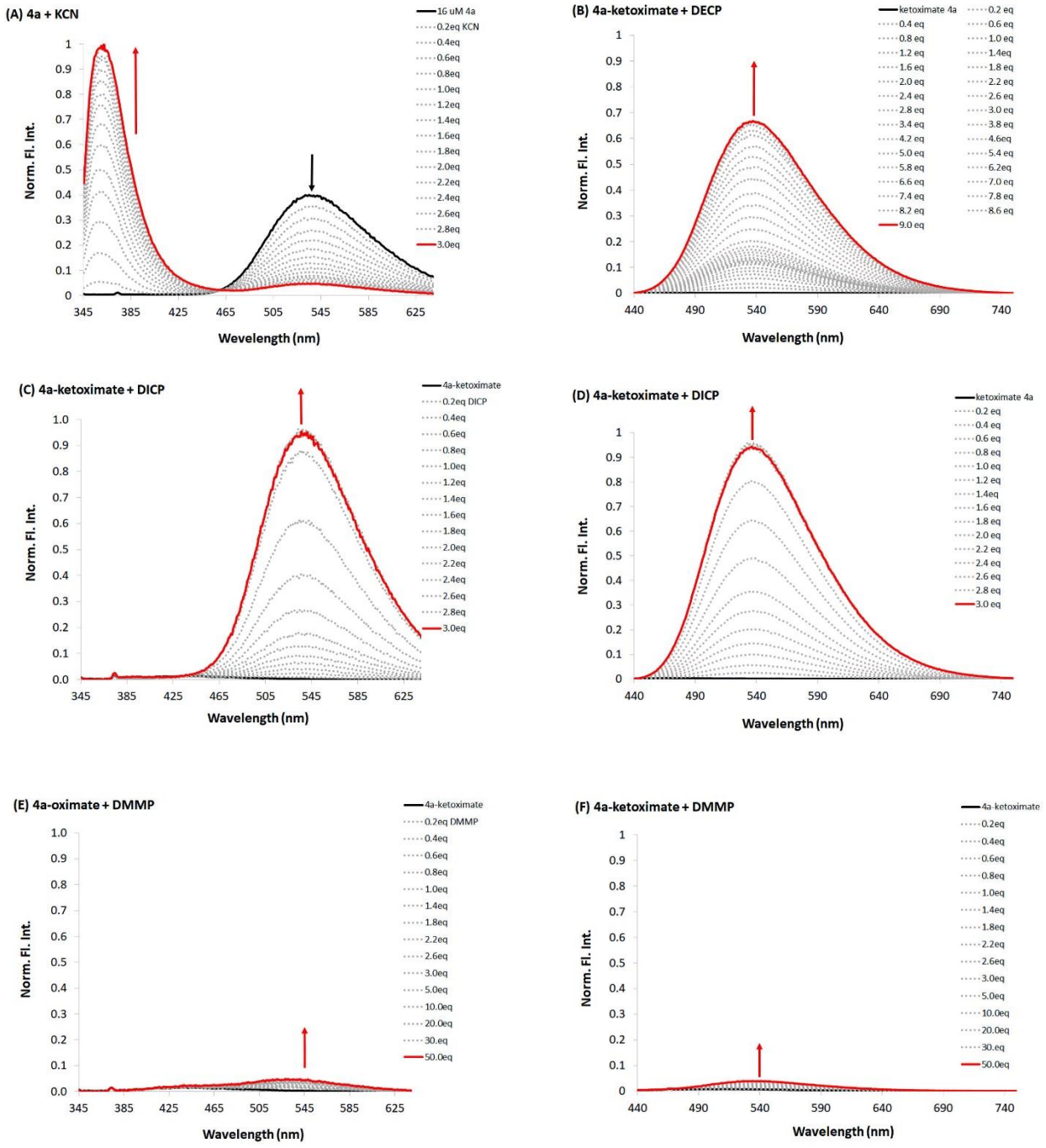

Figure S22. Steady-state fluorescence titration of **4a** (16 μmol·dm^{-3}, DMSO, 298 K). Excited at 336 nm (Black; A, C & E) and excited at 410 nm (Gray; B, D & F).

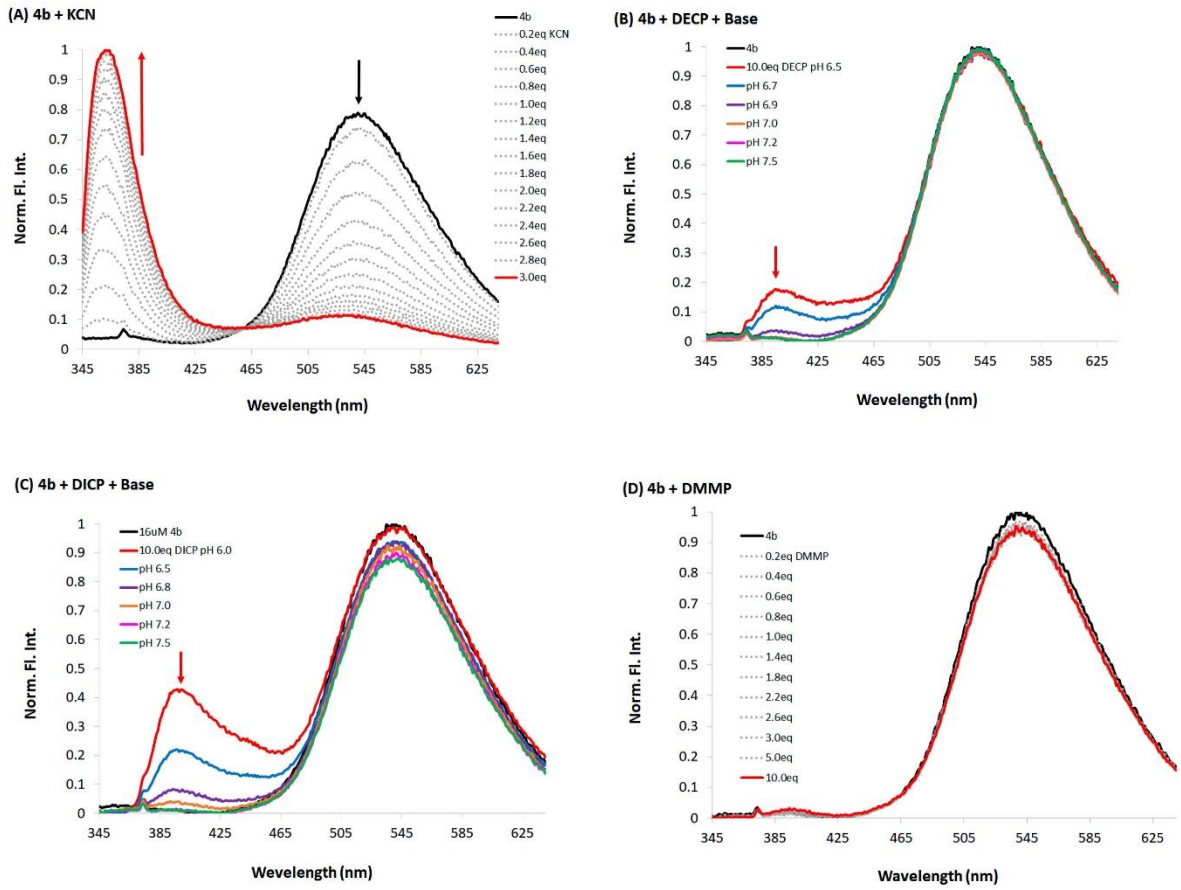

Figure S23. Steady-state fluorescence titration of of **4b** (16 μmol·dm^{-3} λ_{ex} = 336 nm, DMSO, 298 K). (B & C) ten equivalence base (P_4-*t*-Bu) added to 'mop up' excess acid.

4. Fluorescence Lifetime of 4a, 4a-oximate and adducts and model systems

Lifetime fluorescence was performed using 300 nm NanoLED LESER light source with emission set to 540 nm.

4a+KCN

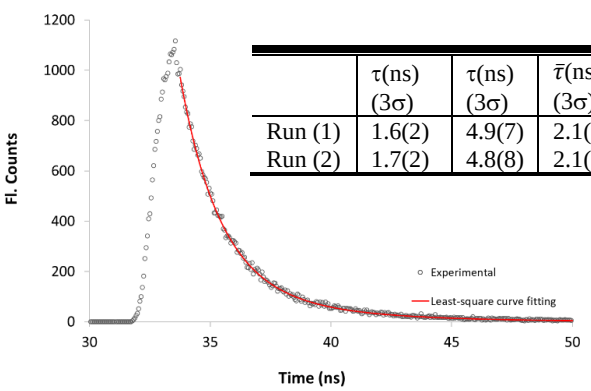

	τ(ns) (3σ)	τ(ns) (3σ)	$\bar{\tau}$(ns) (3σ)	A (3σ)	χ^2
Run (1)	1.6(2)	4.9(7)	2.1(7)	0.4(4)	1.07
Run (2)	1.7(2)	4.8(8)	2.1(8)	0.6(5)	1.01

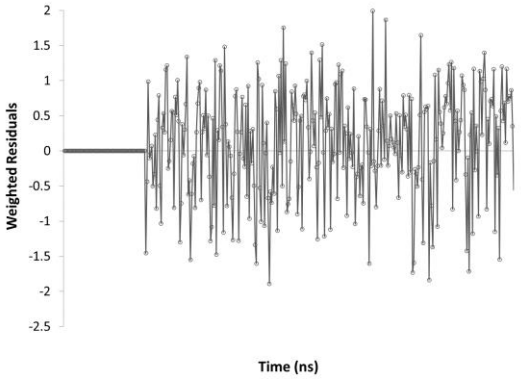

4a-ketoximate+DICP

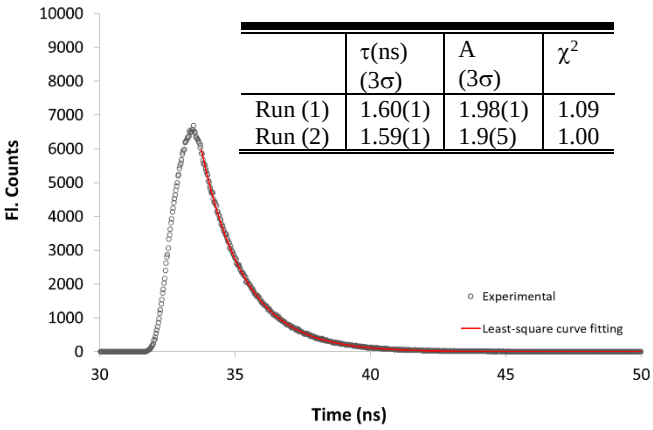

	τ(ns) (3σ)	A (3σ)	χ^2
Run (1)	1.60(1)	1.98(1)	1.09
Run (2)	1.59(1)	1.9(5)	1.00

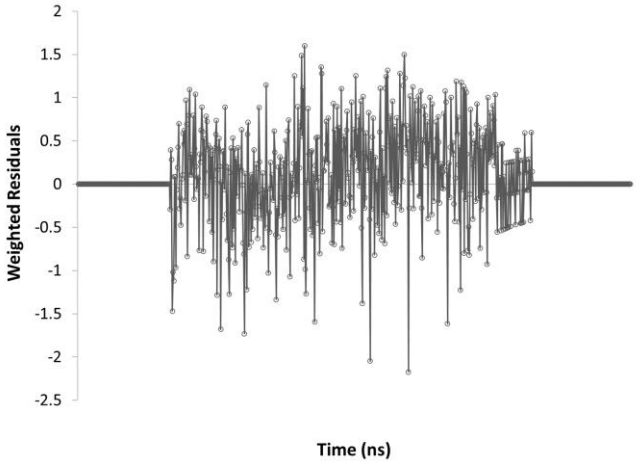

4a-ketoxime+DMMP

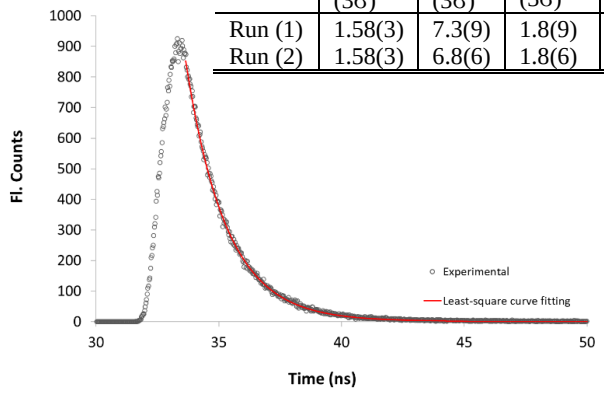

	τ(ns) (3σ)	τ(ns) (3σ)	$\bar{\tau}$(ns) (3σ)	A (3σ)	χ^2
Run (1)	1.58(3)	7.3(9)	1.8(9)	2.6(5)	1.07
Run (2)	1.58(3)	6.8(6)	1.8(6)	3.1(3)	1.09

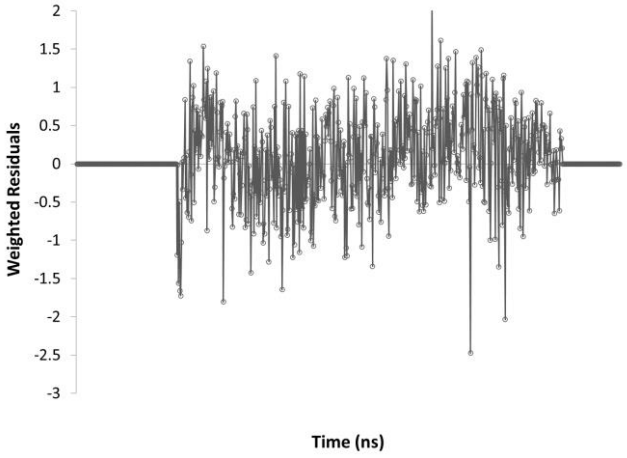

Figure S24. The fluorescence lifetime of **4a**-ketoxime, **4a**-ketoximate (16 μmol·dm^{-3}, DMSO, λ_{em} = 540 nm, 298 K) and upon the addition of KCN, DICP, DMMP. LESER 300 nm light source.

4b

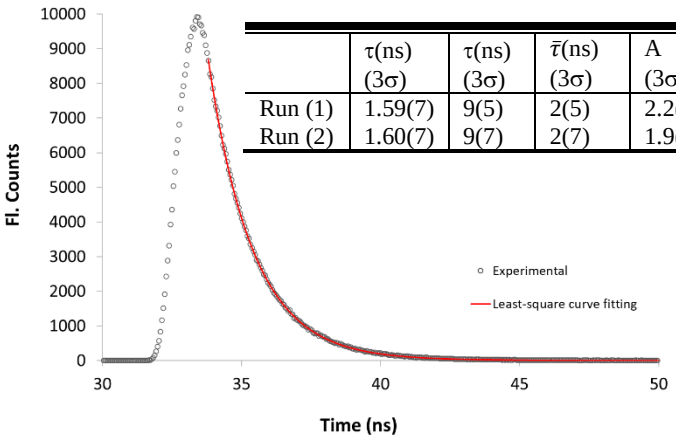

	τ(ns) (3σ)	τ(ns) (3σ)	$\bar{\tau}$(ns) (3σ)	A (3σ)	χ^2
Run (1)	1.59(7)	9(5)	2(5)	2.2(6)	1.09
Run (2)	1.60(7)	9(7)	2(7)	1.9(5)	1.03

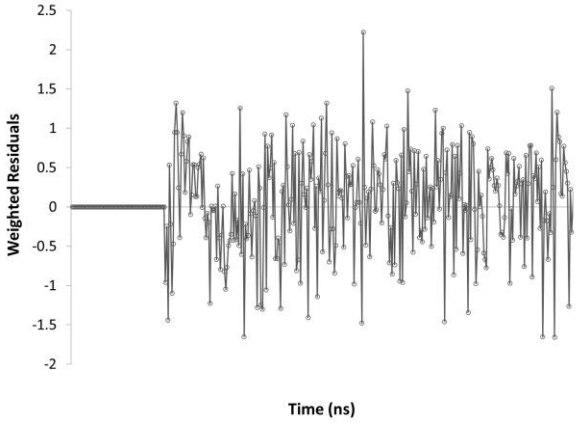

4b + DECP

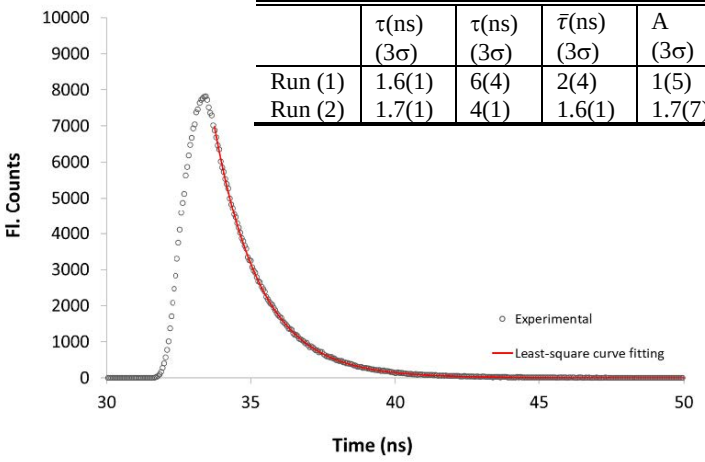

	τ(ns) (3σ)	τ(ns) (3σ)	$\bar{\tau}$(ns) (3σ)	A (3σ)	χ^2
Run (1)	1.6(1)	6(4)	2(4)	1(5)	1.11
Run (2)	1.7(1)	4(1)	1.6(1)	1.7(7)	1.18

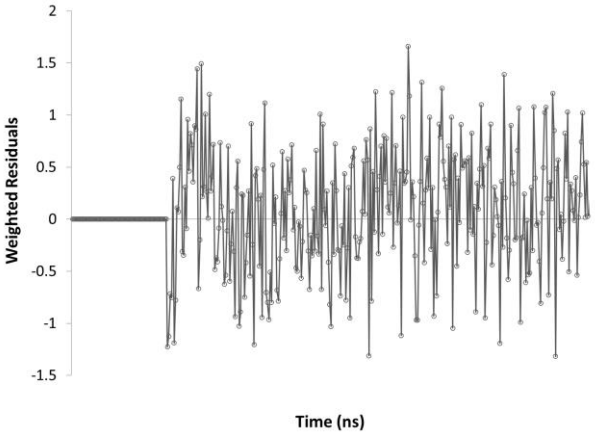

4b+KCN

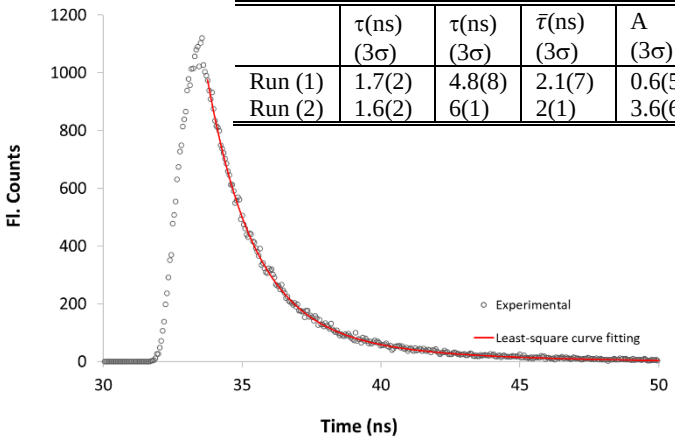

	τ(ns) (3σ)	τ(ns) (3σ)	$\bar{\tau}$(ns) (3σ)	A (3σ)	χ^2
Run (1)	1.7(2)	4.8(8)	2.1(7)	0.6(5)	1.01
Run (2)	1.6(2)	6(1)	2(1)	3.6(6)	1.00

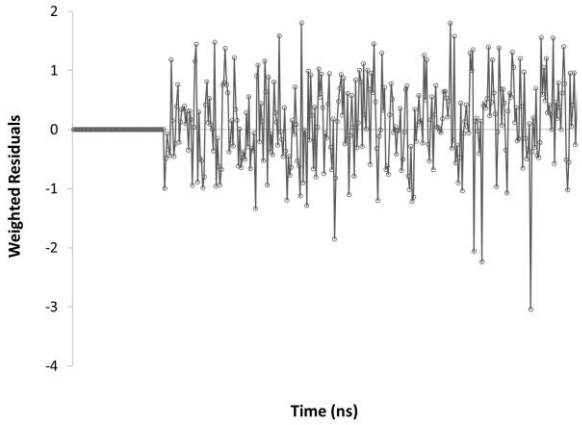

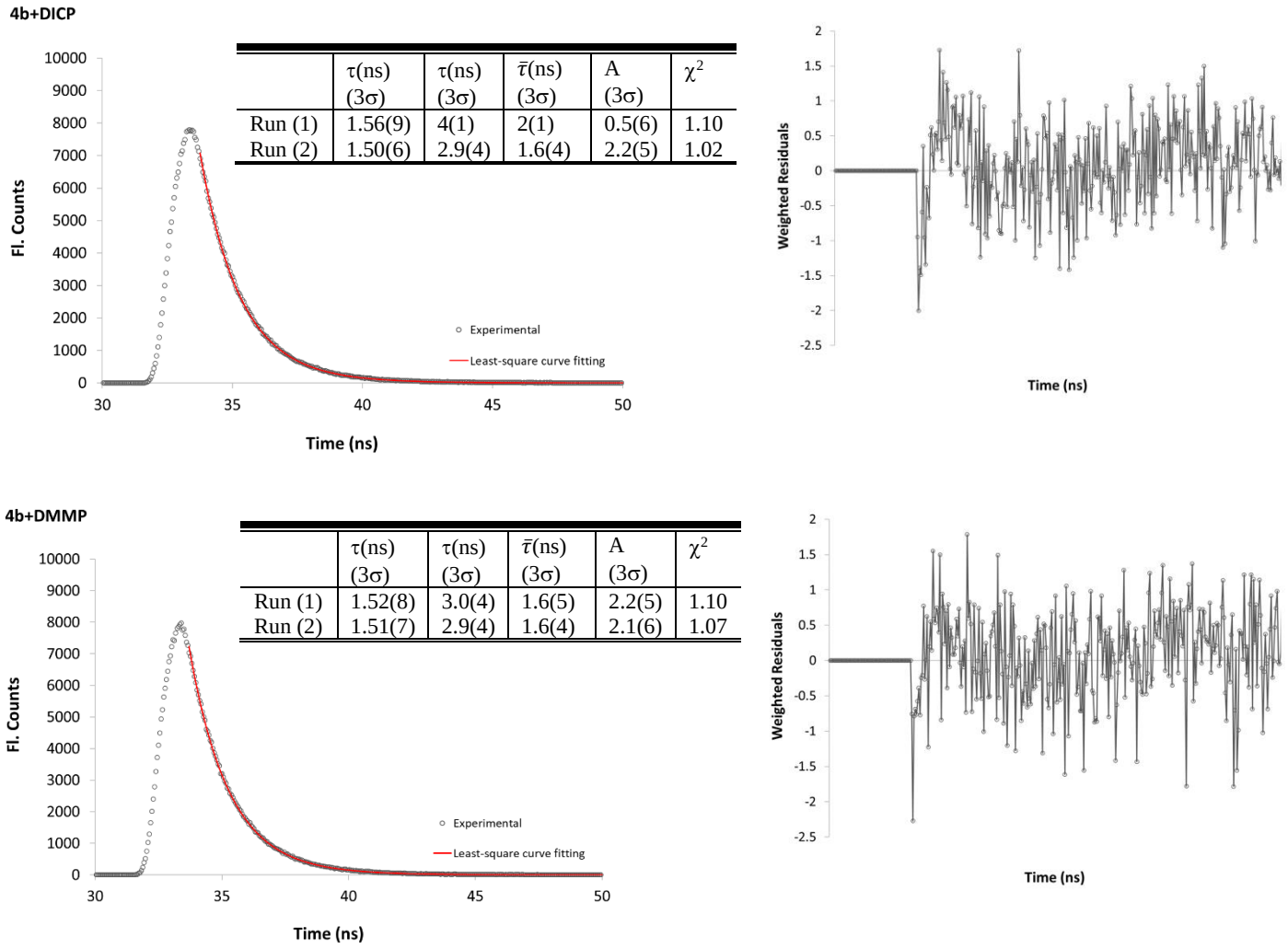

	τ(ns) (3σ)	τ(ns) (3σ)	$\bar{\tau}$(ns) (3σ)	A (3σ)	χ^2
Run (1)	1.56(9)	4(1)	2(1)	0.5(6)	1.10
Run (2)	1.50(6)	2.9(4)	1.6(4)	2.2(5)	1.02

	τ(ns) (3σ)	τ(ns) (3σ)	$\bar{\tau}$(ns) (3σ)	A (3σ)	χ^2
Run (1)	1.52(8)	3.0(4)	1.6(5)	2.2(5)	1.10
Run (2)	1.51(7)	2.9(4)	1.6(4)	2.1(6)	1.07

Figure S25. Fluorescence lifetime of **4b** (16 μmol·dm^{-3}, DMSO, λ_{em} = 540 nm, 298 K) and upon the addition of DECP, KCN, DICP, DMMP using 300 nm LESER light source.

Table S3. Fluorescence lifetimes (τ) of various reactive species (average of best two run).

	τ_1(ns) (3σ)	τ_2(ns) (3σ)	$\bar{\tau}$(ns) (3σ)	A (3σ)	χ^2
4a	1.61 (1)	N/A	1.61 (1)	2.8 (6)	1.07
4a-oximate	0.9 (2)	6.2 (5)	2.3 (5)	3.8 (4)	1.12
Diethyl phosphorocyanidate (DECP)	1.6(2)	9 (1)	2 (1)	1.2 (4)	1.09
KCN	1.7 (2)	4.9 (±7)	2.1 (7)	0.5 (5)	1.06
Diisopropyl chlorophosphite (DICP)	1.60 (1)	N/A	1.60 (1)	2.0 (2)	1.05
Dimethyl methylphosphonate (DMMP)	1.59 (3)	7.1 (8)	1.8 (8)	2.8 (4)	1.08
4b	1.60 (7)	9 (6)	2 (6)	2.0 (5)	1.06
DECP	1.6 (1)	5 (2)	2 (2)	0.9 (6)	1.15
KCN	1.7 (2)	5 (1)	2 (1)	2.1 (6)	1.01
DICP	1.53 (8)	3.6 (8)	1.6 (8)	1.4 (6)	1.06
DMMP	1.52 (8)	2.9 (4)	1.6 (4)	2.2 (5)	1.09

5. 1D and 2D NMR spectra for 4a plus KCN

Table S4. ^{1}H and ^{13}C NMR assignment for **4a** in DMSO-d_6, 298 K.

	^{1}H NMR (ppm, *J* = Hz)	**^{13}C NMR (ppm)**
2	NA	163.6
3	NA	88.4
4	NA	173.2
4a	NA	150.0
5	7.56 (d, *J* = 8.8, 1H)	125.5
6	6.48 (dd, *J* = 8.9, 2.5, 1H)	106.8
7	NA	111.2
8	6.21 (d, *J* = 2.4, 1H)	96.4
8a	NA	155.6
9	5.63 (*d*, *J* = 9.6, 1H)	40.6
10	NA	146.9
11/11’	6.74 (*d*, *J* = 8.9 2H)	113.0
12/12’	7.46 (*d*, *J* = 8.8, 2H)	126.4
13	NA	126.2
14	NA	152.6
15	2.07 (*s*, 3H)	11.2
16	3.25 (*t*, *J* = 7.7, 4H)	51.9
17	1.54 (h, *J* = 7.39, 7.39, 7.32, 7.32, 7.32, 4H)	20.0
18	0.89 (*t*, *J* = 7.4, 6H)	11.1
OH (oxime)	10.76 (br s, 1H)	NA
NH	6.38 (d, *J* = 9.8, 1H)	NA
CN	NA	120.6

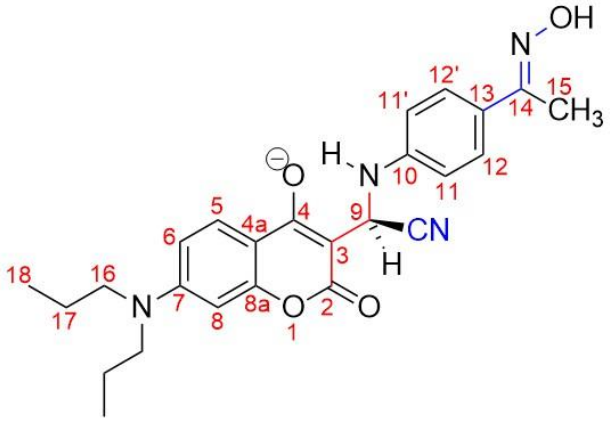

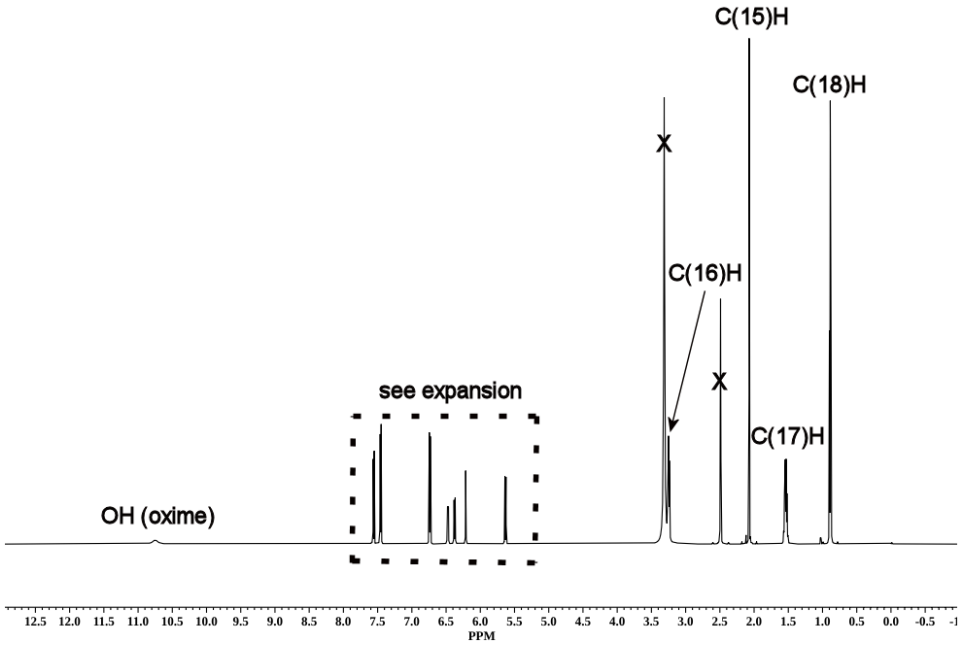

Figure S26. ^{1}H-NMR spectrum of **4a** plus two equivalence KCN in DMSO-d_6 at 298 K.

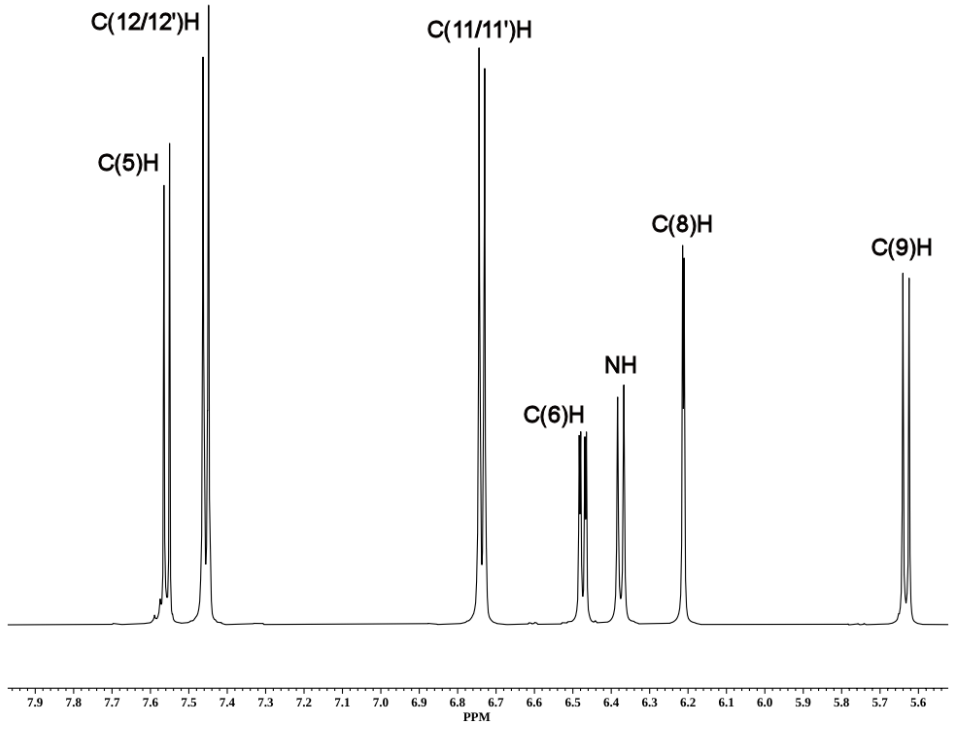

Figure S27. ^{1}H-NMR spectrum (expansion-aromatic region) of **4a** plus two equivalence KCN in DMSO-d_6 at 298 K.

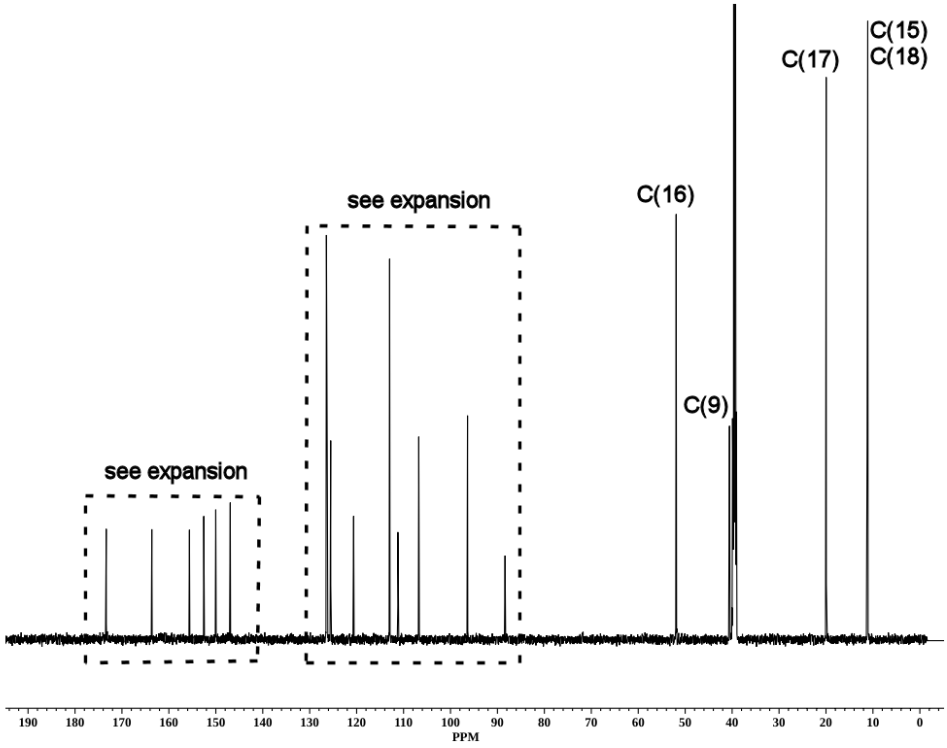

Figure S28. ^{13}C-NMR spectrum of **4a** plus two equivalence KCN in DMSO-d_6 at 298 K.

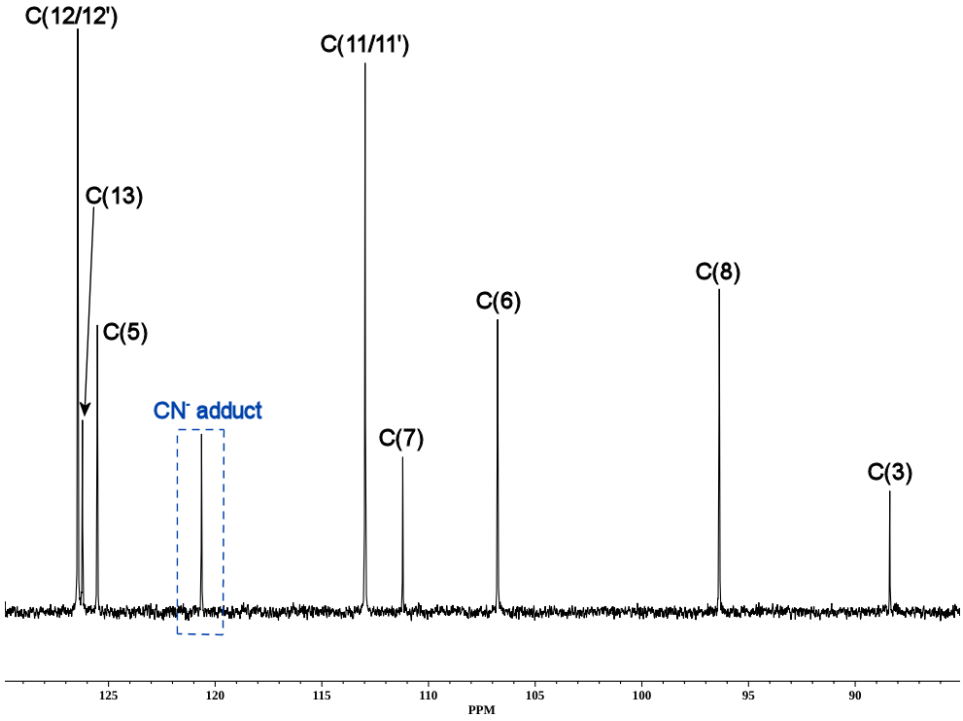

Figure S29. ^{13}C-NMR spectrum (expansion 85 to 130 ppm) of **4a** plus two equivalence KCN in DMSO-d_6 at 298 K.

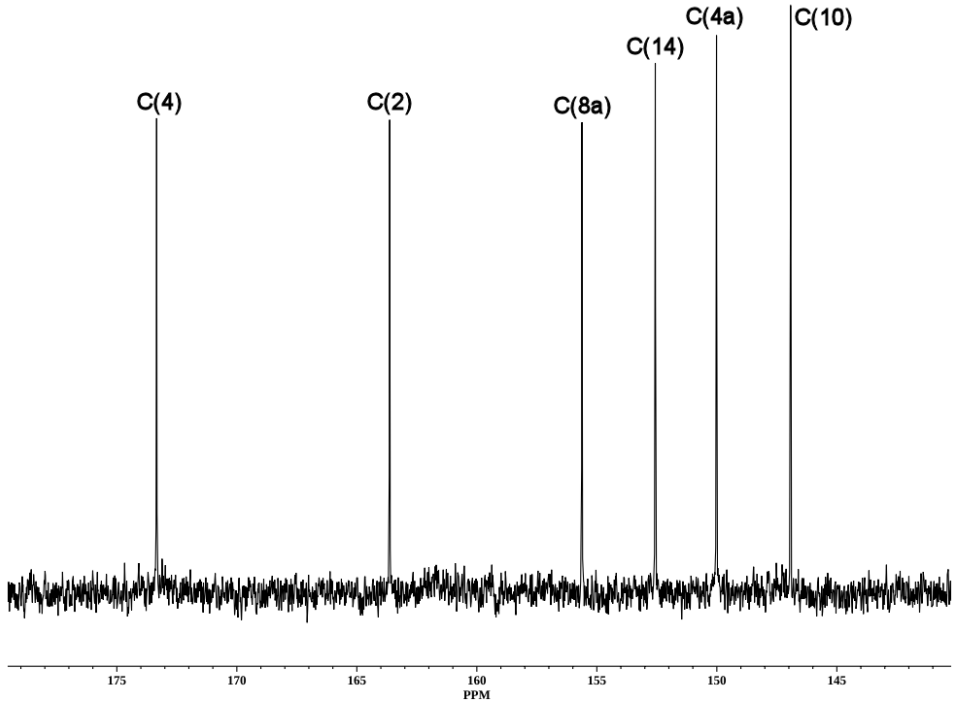

Figure S30. ^{13}C-NMR spectrum (expansion 140 to 180 ppm) of **4a** plus two equivalence KCN in DMSO-d_6 at 298 K.

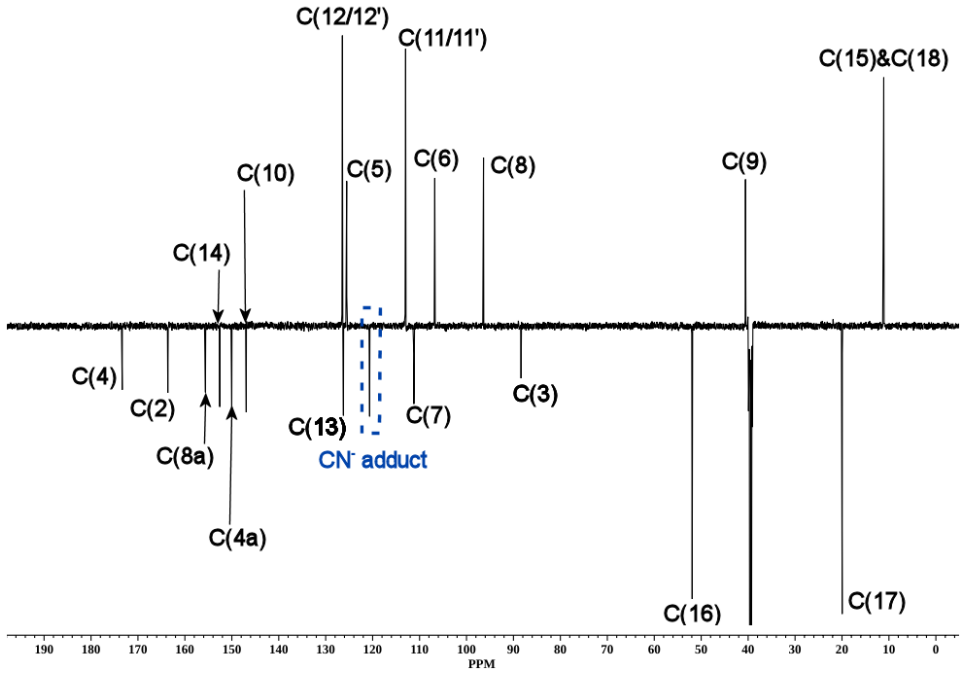

Figure S31. ^{13}C-APT NMR spectrum of **4a** plus two equivalence KCN in DMSO-d_6 at 298 K.

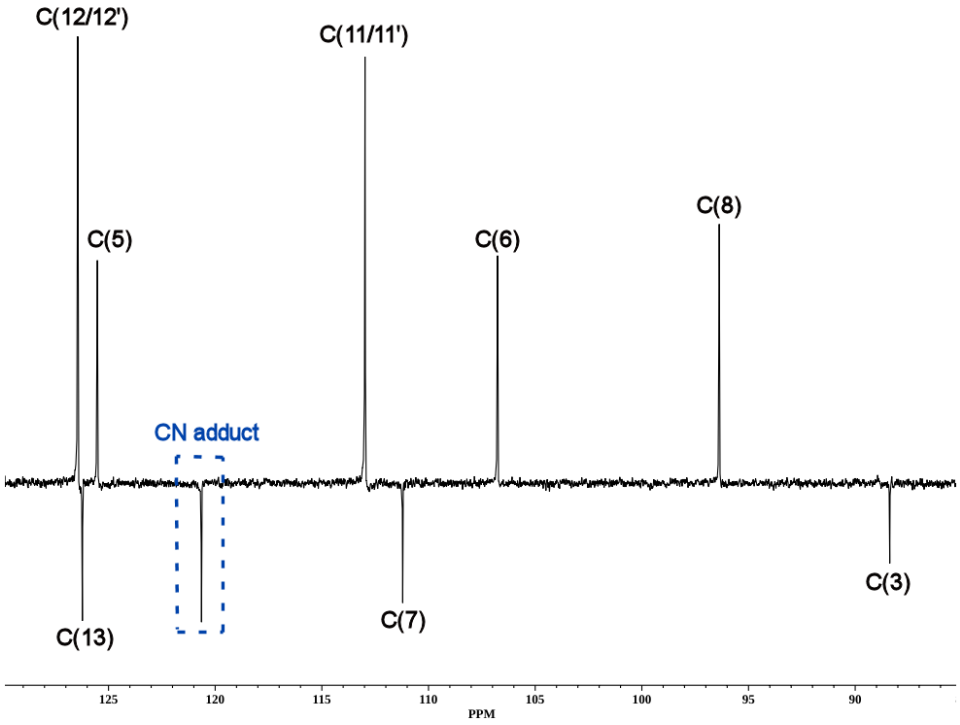

Figure S32. ^{13}C-APT NMR spectrum (expansion 80 to 130 ppm) of **4a** plus two equivalence KCN in DMSO-d_6 at 298 K.

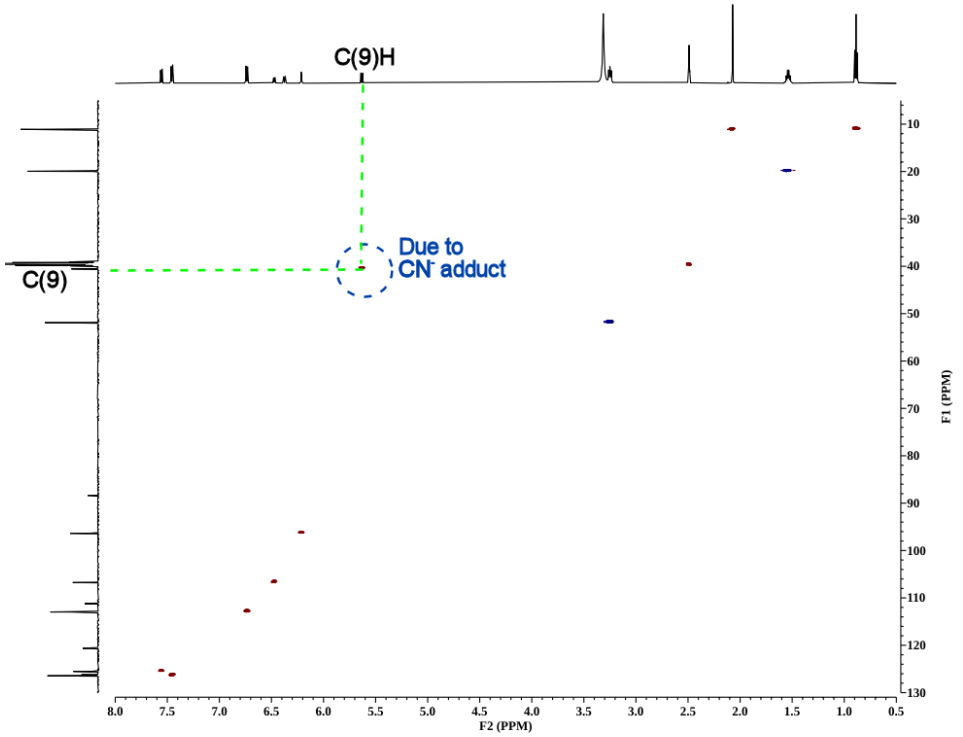

Figure S33. HSQC spectrum (full spectrum) of **4a** plus two equivalence KCN in DMSO-d_6 at 298 K.

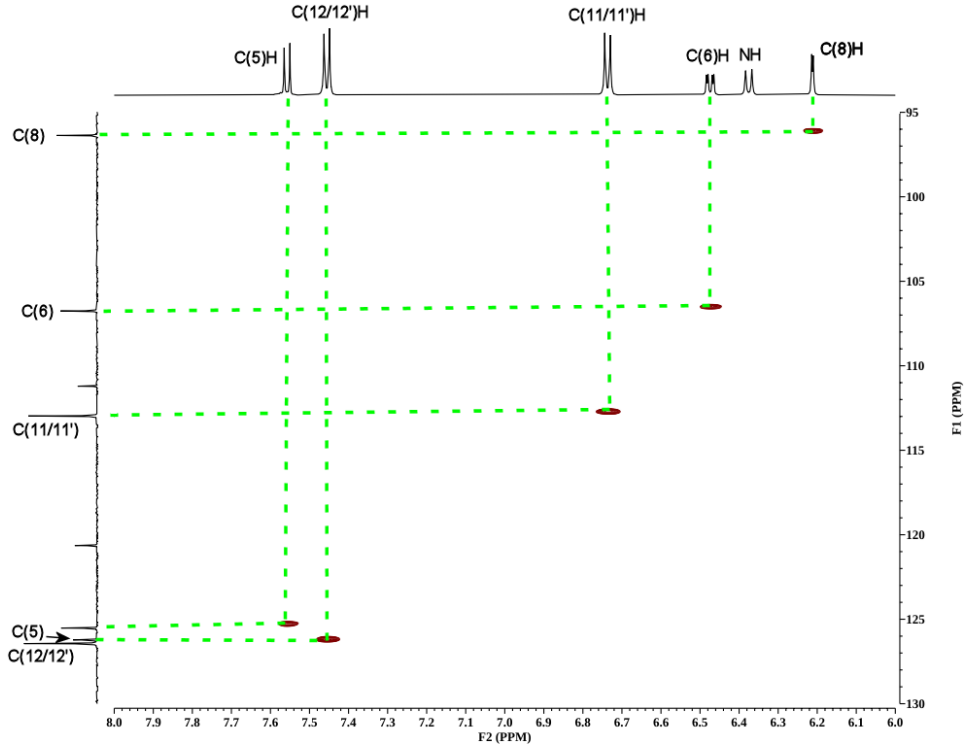

Figure S34. HSQC spectrum (expansion aromatic region) of **4a** plus two equivalence KCN in DMSO-d_6 at 298 K.

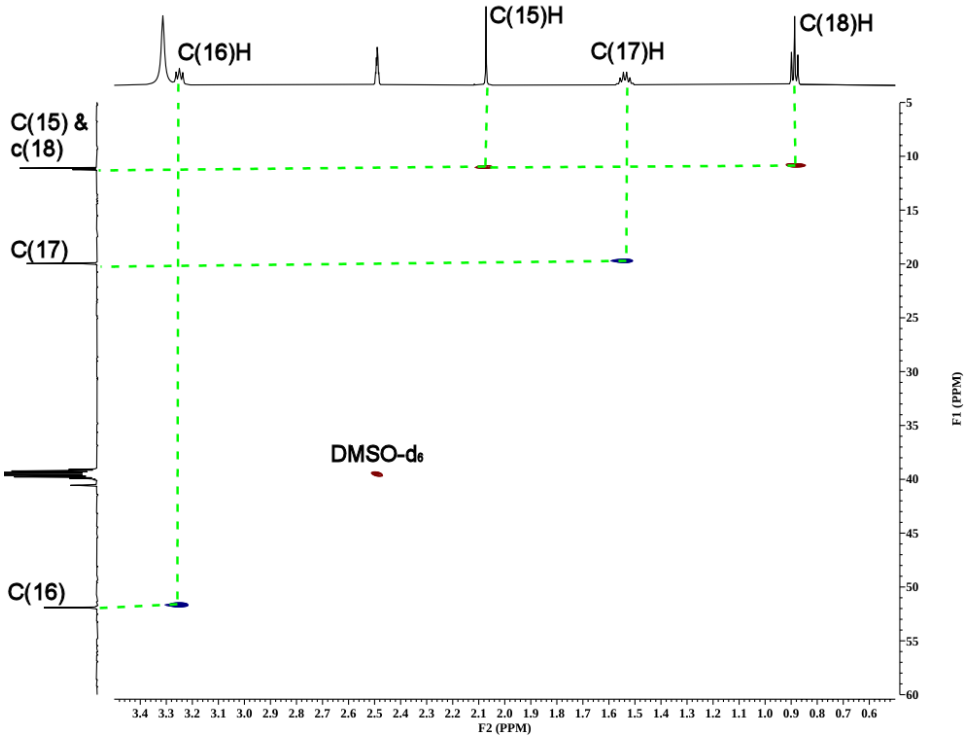

Figure S35. HSQC spectrum (expansion) of **4a** plus two equivalence KCN in DMSO-d_6 at 298 K.

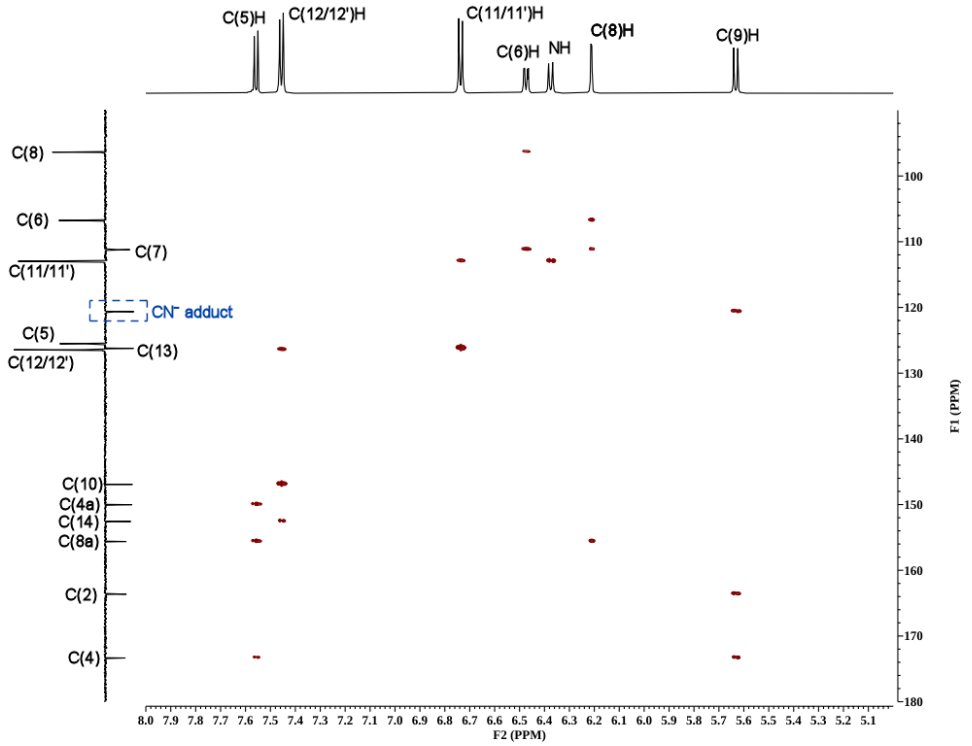

Figure S36. HMBC spectrum (expansion) of **4a** plus two equivalence KCN in DMSO-d_6 at 298 .

6. In situ NMR Experiments; 4a plus DECP

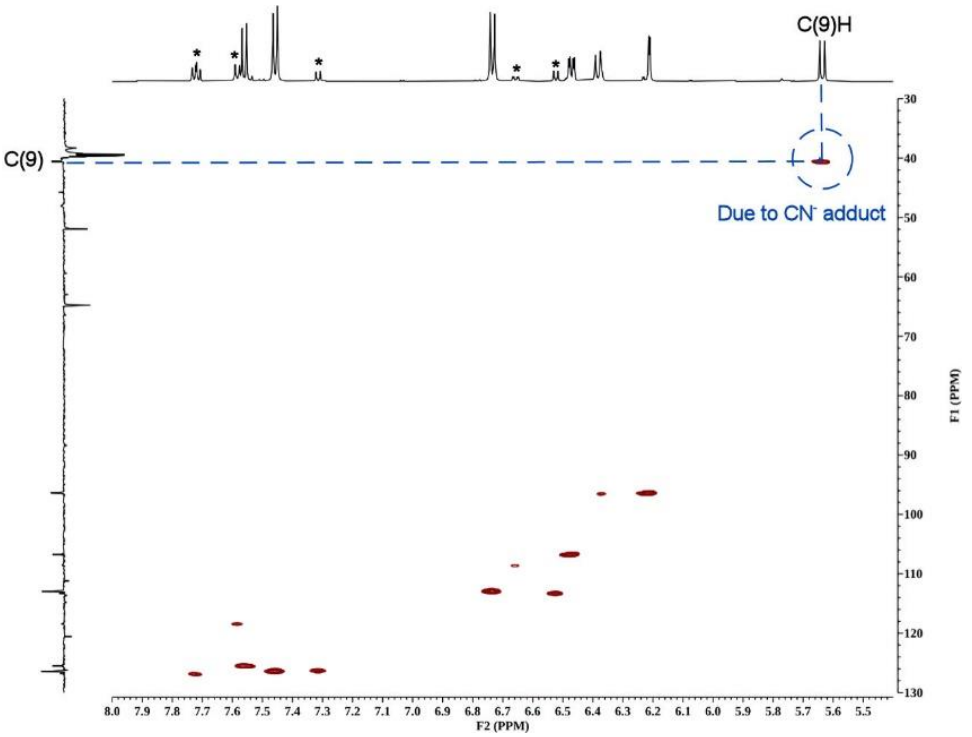

Figure S37. HSQC spectrum (expansion) of **4a** plus Hünig's base plus three equivalence DECP in DMSO-d_6 at 298 K (*) are degraded products.

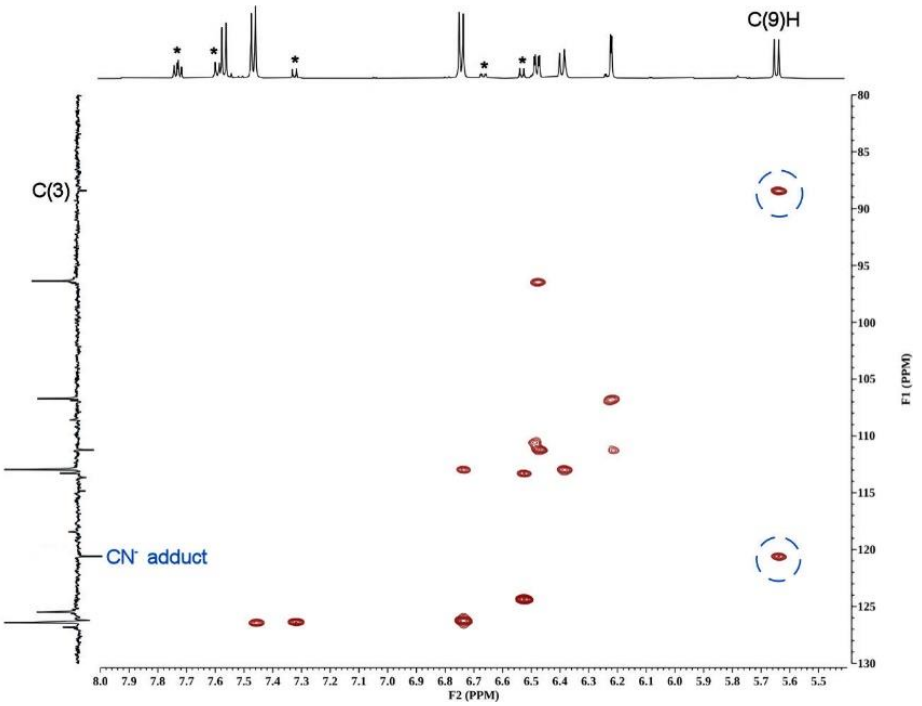

Figure S38. HMBC spectrum (expansion) of **4a** plus Hünig's base plus three equivalence DECP in DMSO-d_6 at 298 K (*) are degraded products.

7. Mass Spectometry of 4a plus DECP

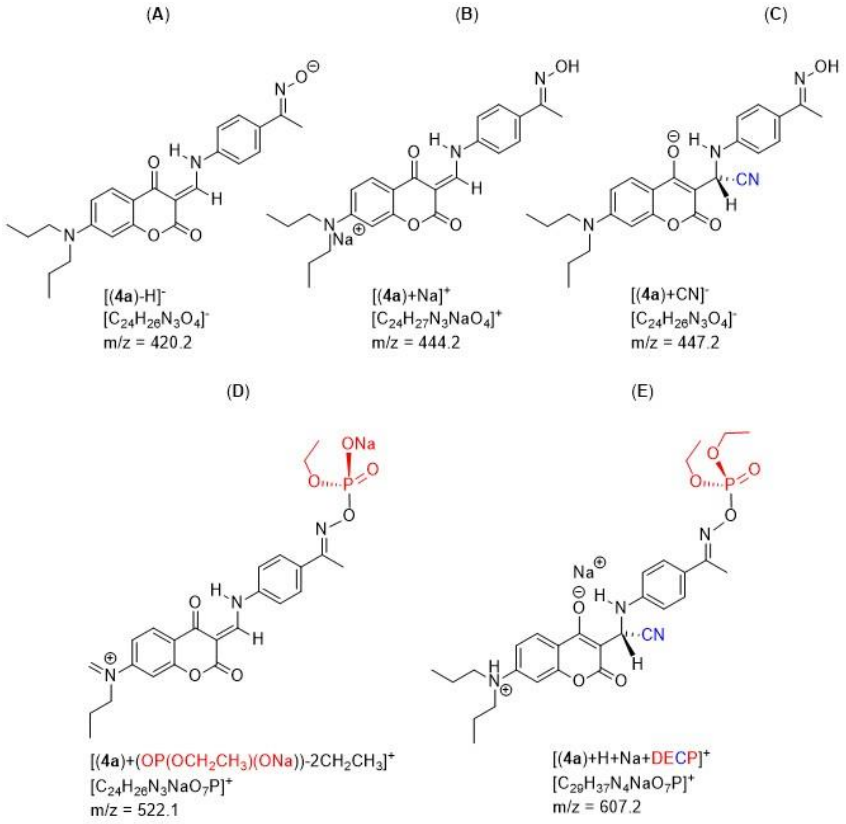

Figure S39. Possible structures assigned to the mass spectroscopy signals (negative and positive mode).

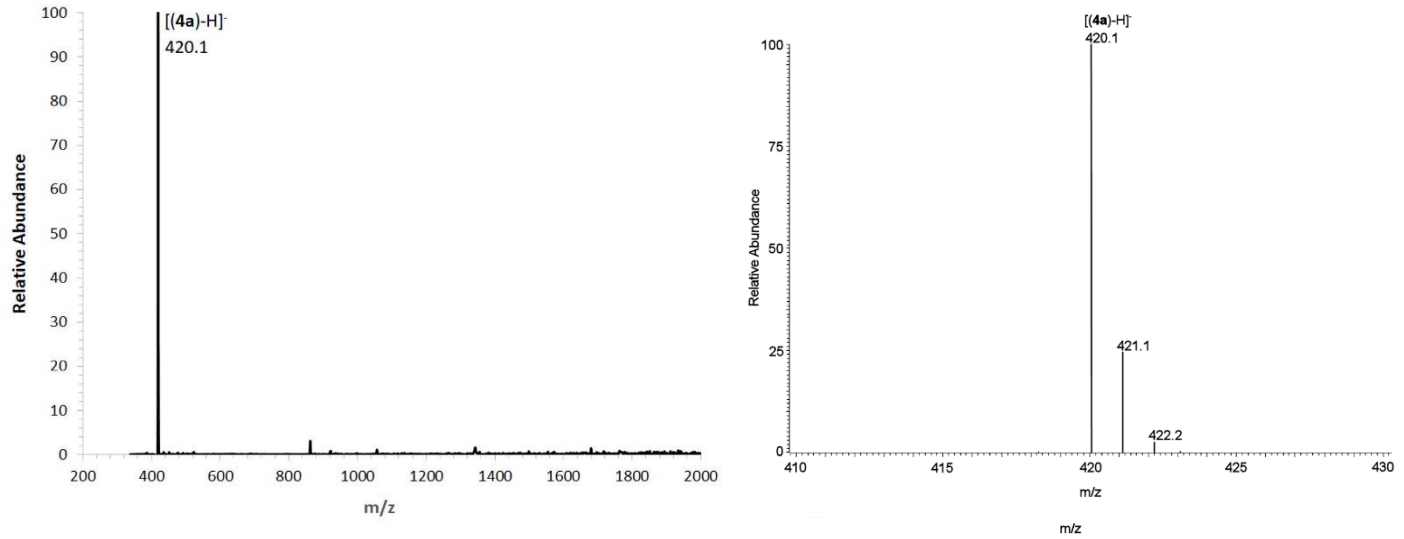

Figure S40. ESI-MS; free **4a** (negative mode) LHS: full spectrum.

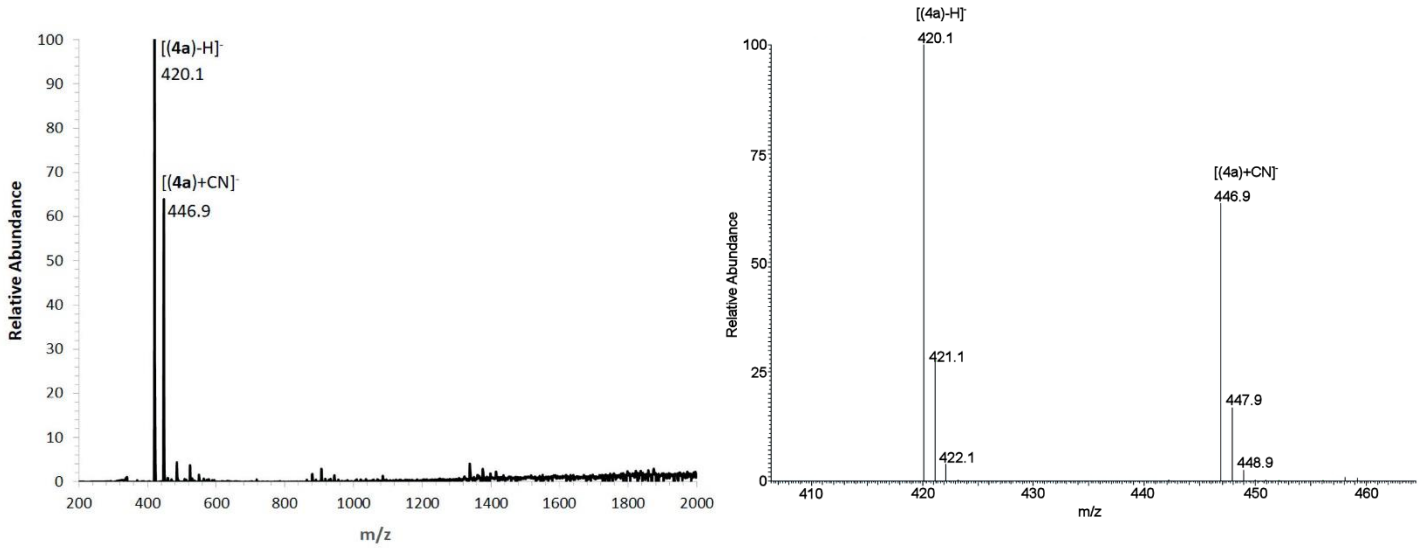

Figure S41. ESI-MS; **4a-CN**$^-$ adduct upon the addition of two equivalence KCN (negative mode); The free **4a** also can be seen at 298K. LHS: full spectrum.

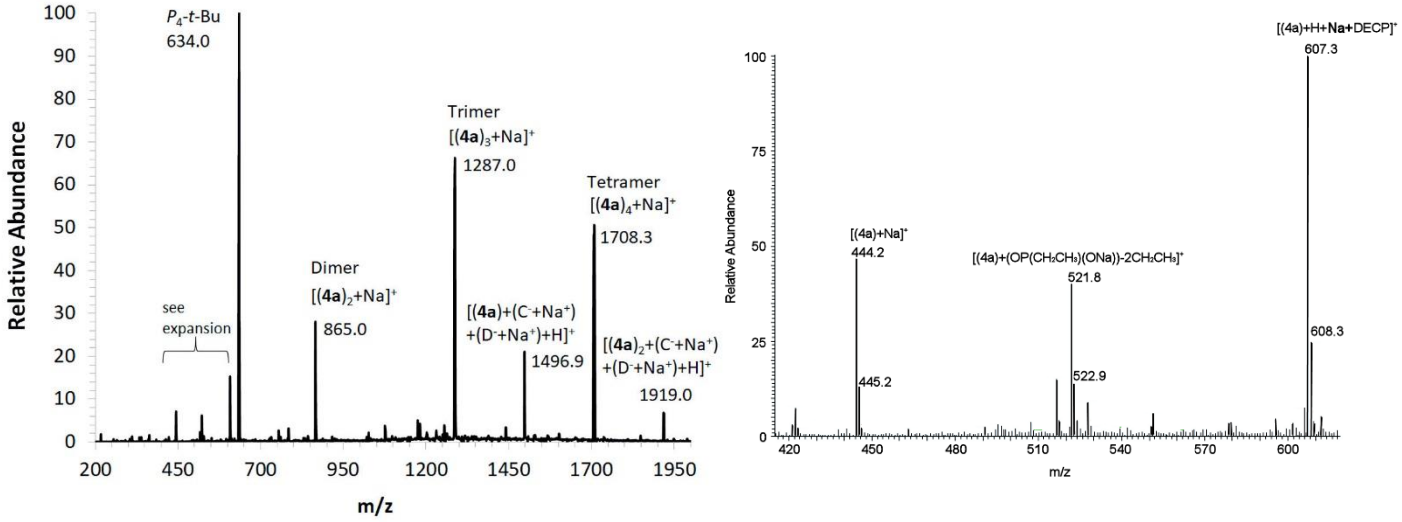

Figure S42. Left: ESI-MS; **4a-DECP** adduct (positive mode); upon the addition of P_4-*t*-Bu and DECP (dimers, trimers, and tetramers of 4a and proposed species are shown in figure S39) are identifiable. Right: To improve the relative abundance of the adducts, we re-run the ESI-MS experiments beteen m/z 200 and 600. The MS shows three distinct speacies are identified **4a**, species (D-fig. S39) and the desired bis-adduct (species E-fig S39), at 298 K.

8. Molecular Modelling

Computational details reported in the manuscript.

tabun mimic	-818.081328 au
ketoximate	-1394.551554 au
(total for reactants	-2212.632882 au)
transition state 1	-2212.496011 au
transition state 2	-2212.583400 au
product	-2212.701827 au

$\Delta E_{(\text{reactants} \rightarrow \text{TS1})}$ = 0.136871 au (+359.29 kJmol^{-1})

$\Delta E_{(\text{TS1} \rightarrow \text{TS2})}$ = -0.0873789 au (-229.37 kJmol^{-1})

$\Delta E_{(\text{TS2} \rightarrow \text{product})}$ = -0.118427 au (-310.87 kJmol^{-1})

$\Delta E_{(\text{reactants} \rightarrow \text{product})}$ = -0.068945 au (-180.95 kJmol^{-1})

9. Limit of Detection

The LOD was determined by least square linear regression. Confidence limit of the slope is defined as $b \pm t_{sb}$ where t is the t value obtained from 95% confidence level (n = 12; t = 1.782). It is accepted that the LOD is the analyte concentration giving a signal equal to that of the blank signal plus three standard deviations from the blank ($y = y_b + 3S_b$).

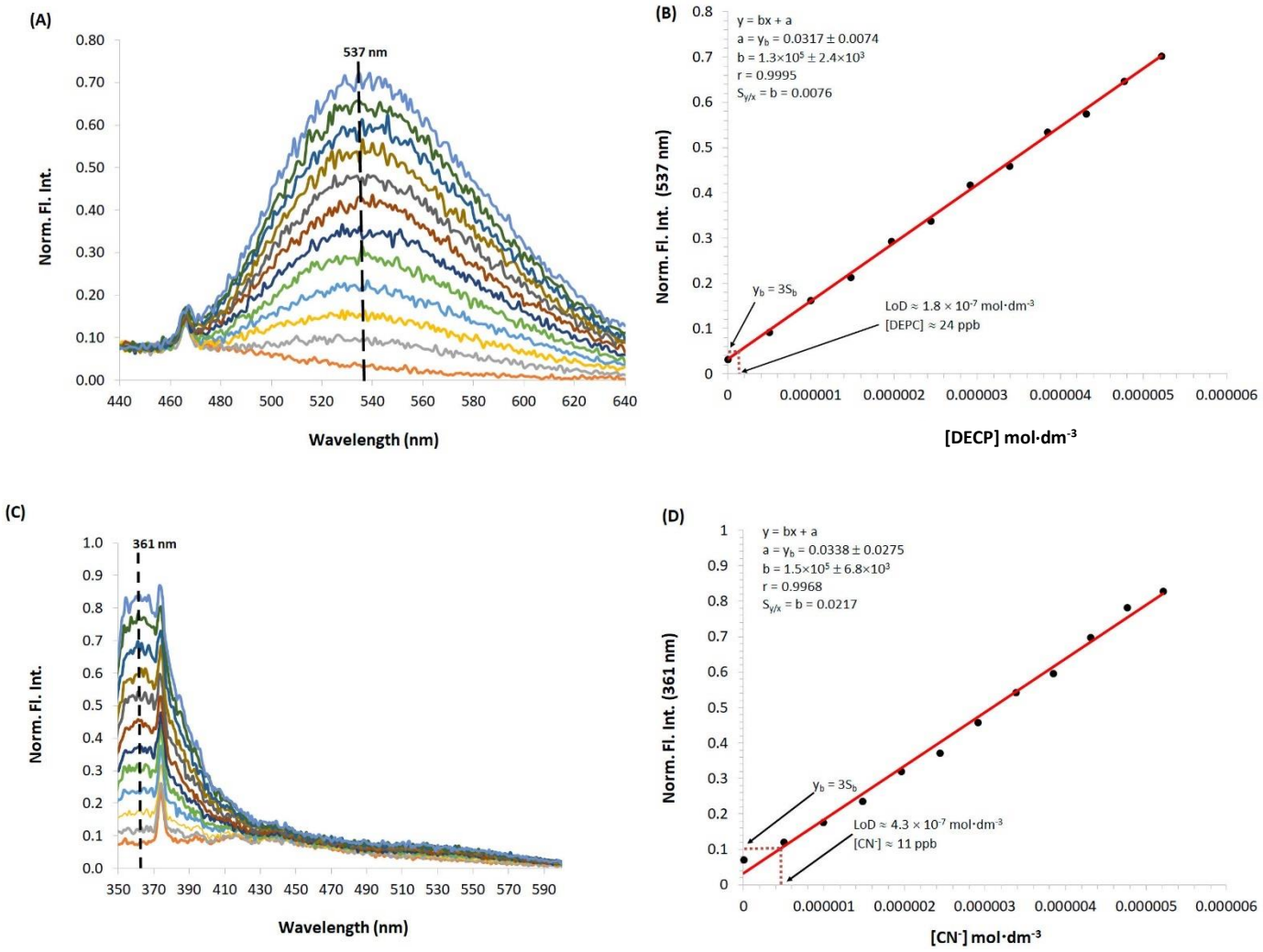

Figure S43. Limit of detection of Chemodosimeter **4a** on the addition of DECP (A) Normalized fluorescence spectra of **4a**-DECP adduct (B) Linear regression fit, (C) Normalized fluorescence graph of **4a**-cyanide adduct (D) Linear regression fit in DMSO (1.0 μM, λex = 440 nm and λex = 336 nm for (A) and (C), respectively at 298 K).

10.0 X-ray crystallographic Tables

Computing details

Data collection: Bruker *APEX3*; cell refinement: Bruker *SAINT*; data reduction: Bruker *SAINT*; program(s) used to solve structure: *SHELXT* 2014/5 (Sheldrick, 2014); program(s) used to refine structure: *SHELXL2017*/1 (Sheldrick, 2017).

Compound 4a

Crystal data

$C_{24}H_{27}N_3O_4$
$M_r = 421.48$
Triclinic, $P\overline{1}$
$a = 5.1039$ (3) Å
$b = 14.0847$ (8) Å
$c = 15.9717$ (9) Å
$\alpha = 69.320$ (4)°
$\beta = 87.965$ (5)°
$\gamma = 80.713$ (4)°
$V = 1059.81$ (11) Å^3
$Z = 2$
$F(000) = 448$
$D_x = 1.321$ Mg m^{-3}
Cu $K\alpha$ radiation, $\lambda = 1.54184$ Å
Cell parameters from 926 reflections
$\theta = 3.0$–$58.1°$
$\mu = 0.74$ mm^{-1}
$T = 90$ K
Needle, yellow
0.24 × 0.03 × 0.01 mm

Data collection

Bruker Kappa APEX-II DUO diffractometer
Radiation source: IμS microfocus
QUAZAR multilayer optics monochromator
φ and ω scans
Absorption correction: multi-scan *SADABS* (Krause *et al.*, 2015)
$T_{min} = 0.714$, $T_{max} = 0.993$
9299 measured reflections
3045 independent reflections
1468 reflections with $I > 2\sigma(I)$
$R_{int} = 0.120$
$\theta_{max} = 59.0°$, $\theta_{min} = 3.0°$
$h = -5 \rightarrow 5$
$k = -15 \rightarrow 15$
$l = -17 \rightarrow 17$

Refinement

Refinement on F^2
Least-squares matrix: full
$R[F^2 > 2\sigma(F^2)] = 0.078$
$wR(F^2) = 0.236$
$S = 0.95$
3045 reflections
288 parameters
0 restraints
Hydrogen site location: mixed
H atoms treated by a mixture of independent and constrained refinement
$w = 1/[\sigma^2(F_o^2) + (0.1078P)^2]$ where $P = (F_o^2 + 2F_c^2)/3$
$(\Delta/\sigma)_{max} < 0.001$
$\Delta\rho_{max} = 0.31$ e Å^{-3}
$\Delta\rho_{min} = -0.30$ e Å^{-3}
Extinction correction: *SHELXL2017*/1 (Sheldrick 2017), $Fc^* = kFc[1+0.001xFc^2\lambda^3/\sin(2\theta)]^{-1/4}$
Extinction coefficient: 0.0035 (10)

Special details

Geometry. All e.s.d.'s (except the e.s.d. in the dihedral angle between two l.s. planes) are estimated using the full covariance matrix. The cell e.s.d.'s are taken into account individually in the estimation of e.s.d.'s in distances, angles and torsion angles; correlations between e.s.d.'s in cell parameters are only used when they are defined by crystal symmetry. An approximate (isotropic) treatment of cell e.s.d.'s is used for estimating e.s.d.'s involving l.s. planes.

Fractional atomic coordinates and isotropic or equivalent isotropic displacement parameters (Å²)

	x	*y*	*z*	U_{iso}*/U_{eq}
O1	−0.0788 (7)	0.4304 (3)	0.6492 (2)	0.0468 (10)
O2	0.2337 (7)	0.4963 (3)	0.5600 (2)	0.0508 (10)
O3	0.1501 (7)	0.1488 (3)	0.6235 (2)	0.0488 (10)
O4	1.6292 (7)	0.0299 (3)	0.2504 (2)	0.0509 (10)
N1	0.5043 (9)	0.2310 (4)	0.5091 (3)	0.0481 (12)
N2	1.4189 (8)	0.0474 (3)	0.3061 (3)	0.0476 (12)
N3	−0.7598 (8)	0.3124 (3)	0.8508 (3)	0.0497 (12)
C2	0.1317 (10)	0.4204 (4)	0.5935 (3)	0.0446 (13)
C3	0.2045 (10)	0.3222 (4)	0.5827 (3)	0.0446 (13)
C4	0.0814 (10)	0.2354 (4)	0.6309 (4)	0.0444 (13)
C4A	−0.1334 (10)	0.2517 (4)	0.6891 (3)	0.0462 (14)
C5	−0.2727 (10)	0.1752 (4)	0.7397 (3)	0.0500 (14)
H5	−0.227347	0.108428	0.736548	0.060*
C6	−0.4752 (11)	0.1926 (4)	0.7944 (4)	0.0514 (15)
H6	−0.564038	0.137790	0.829246	0.062*
C7	−0.5524 (10)	0.2929 (4)	0.7991 (3)	0.0474 (14)
C8	−0.4099 (10)	0.3699 (4)	0.7479 (3)	0.0499 (15)
H8	−0.453032	0.437275	0.749783	0.060*
C8A	−0.2071 (10)	0.3483 (4)	0.6947 (3)	0.0446 (13)
C9	0.4116 (10)	0.3173 (4)	0.5241 (3)	0.0481 (14)
H9	0.488453	0.377199	0.494113	0.058*
C10	0.7095 (10)	0.2159 (4)	0.4498 (3)	0.0451 (13)
C11	0.8530 (11)	0.2908 (5)	0.4014 (4)	0.0517 (15)
H11	0.816318	0.357654	0.404868	0.062*
C11A	0.7595 (11)	0.1188 (4)	0.4452 (3)	0.0499 (14)
H11A	0.659869	0.067456	0.479689	0.060*
C12	1.0538 (11)	0.2671 (4)	0.3472 (4)	0.0494 (14)
H12	1.154779	0.318520	0.313696	0.059*
C12A	0.9573 (10)	0.0964 (4)	0.3895 (3)	0.0476 (14)
H12A	0.988212	0.030209	0.384674	0.057*
C13	1.1096 (10)	0.1698 (4)	0.3410 (3)	0.0452 (14)
C14	1.3299 (10)	0.1438 (4)	0.2855 (3)	0.0445 (14)
C15	1.4469 (11)	0.2280 (4)	0.2161 (4)	0.0563 (16)
H15A	1.560776	0.199267	0.177356	0.084*
H15B	1.552583	0.259853	0.245621	0.084*
H15C	1.303735	0.279871	0.180009	0.084*
C16	−0.8801 (11)	0.2306 (5)	0.9142 (4)	0.0559 (16)
H16A	−0.910694	0.181759	0.885129	0.067*
H16B	−1.055195	0.260267	0.930479	0.067*
C16A	−0.8491 (10)	0.4164 (4)	0.8489 (4)	0.0513 (15)
H16C	−1.037958	0.422370	0.865753	0.062*
H16D	−0.839236	0.464459	0.786710	0.062*
C17	−0.7122 (12)	0.1715 (5)	1.0000 (4)	0.0637 (17)
H17A	−0.540166	0.138940	0.984326	0.076*
H17B	−0.675137	0.220524	1.028071	0.076*
C17A	−0.6942 (11)	0.4506 (5)	0.9099 (4)	0.0566 (16)
H17C	−0.703942	0.403676	0.972578	0.068*
H17D	−0.505263	0.446324	0.893145	0.068*
C18	−0.8478 (13)	0.0896 (5)	1.0667 (4)	0.0743 (19)

H18A	−1.017294	0.121517	1.083097	0.111*
H18B	−0.733840	0.054565	1.120377	0.111*
H18C	−0.880117	0.039655	1.039944	0.111*
C18A	−0.8033 (12)	0.5598 (4)	0.9034 (4)	0.0612 (17)
H18D	−0.795069	0.606263	0.841313	0.092*
H18E	−0.697151	0.580171	0.942203	0.092*
H18F	−0.988237	0.563510	0.922371	0.092*
H4O	1.715 (13)	−0.037 (5)	0.283 (4)	0.092*
H1N	0.423 (12)	0.182 (5)	0.542 (4)	0.073*

Atomic displacement parameters (Å²)

	U^{11}	U^{22}	U^{33}	U^{12}	U^{13}	U^{23}
O1	0.048 (2)	0.046 (2)	0.045 (2)	−0.0051 (17)	0.0013 (18)	−0.0145 (18)
O2	0.052 (2)	0.047 (2)	0.052 (2)	−0.0075 (19)	0.0055 (18)	−0.0153 (19)
O3	0.052 (2)	0.038 (2)	0.055 (2)	−0.0048 (18)	0.0073 (18)	−0.0164 (19)
O4	0.050 (2)	0.045 (2)	0.057 (2)	−0.0036 (18)	0.0113 (19)	−0.0193 (19)
N1	0.049 (3)	0.042 (3)	0.050 (3)	−0.001 (2)	0.002 (2)	−0.014 (2)
N2	0.045 (3)	0.045 (3)	0.052 (3)	−0.003 (2)	0.008 (2)	−0.018 (2)
N3	0.047 (3)	0.047 (3)	0.048 (3)	−0.006 (2)	0.009 (2)	−0.010 (2)
C2	0.044 (3)	0.050 (4)	0.037 (3)	−0.005 (3)	0.004 (3)	−0.014 (3)
C3	0.039 (3)	0.049 (3)	0.044 (3)	−0.002 (3)	0.002 (3)	−0.016 (3)
C4	0.039 (3)	0.039 (3)	0.053 (3)	−0.001 (3)	−0.008 (3)	−0.015 (3)
C4A	0.040 (3)	0.047 (4)	0.048 (3)	−0.007 (3)	−0.002 (3)	−0.012 (3)
C5	0.051 (3)	0.046 (4)	0.049 (3)	−0.005 (3)	0.000 (3)	−0.013 (3)
C6	0.051 (3)	0.048 (4)	0.051 (3)	−0.009 (3)	0.004 (3)	−0.011 (3)
C7	0.045 (3)	0.054 (4)	0.041 (3)	−0.008 (3)	0.000 (3)	−0.014 (3)
C8	0.049 (3)	0.052 (4)	0.046 (3)	0.003 (3)	−0.002 (3)	−0.017 (3)
C8A	0.046 (3)	0.039 (3)	0.043 (3)	−0.009 (3)	0.003 (3)	−0.007 (3)
C9	0.044 (3)	0.049 (4)	0.046 (3)	−0.002 (3)	−0.005 (3)	−0.012 (3)
C10	0.040 (3)	0.050 (4)	0.042 (3)	−0.002 (3)	0.004 (3)	−0.015 (3)
C11	0.050 (3)	0.052 (4)	0.051 (3)	−0.005 (3)	0.000 (3)	−0.018 (3)
C11A	0.053 (3)	0.044 (4)	0.047 (3)	−0.006 (3)	0.004 (3)	−0.009 (3)
C12	0.052 (3)	0.043 (3)	0.050 (3)	−0.004 (3)	0.007 (3)	−0.015 (3)
C12A	0.049 (3)	0.040 (3)	0.049 (3)	−0.007 (3)	0.001 (3)	−0.010 (3)
C13	0.046 (3)	0.046 (3)	0.045 (3)	−0.008 (3)	−0.004 (3)	−0.016 (3)
C14	0.037 (3)	0.048 (4)	0.046 (3)	−0.008 (3)	−0.001 (2)	−0.013 (3)
C15	0.059 (4)	0.050 (4)	0.055 (3)	−0.006 (3)	0.007 (3)	−0.013 (3)
C16	0.050 (3)	0.067 (4)	0.044 (3)	−0.005 (3)	0.007 (3)	−0.015 (3)
C16A	0.037 (3)	0.064 (4)	0.051 (3)	−0.005 (3)	−0.002 (3)	−0.019 (3)
C17	0.059 (4)	0.076 (5)	0.051 (4)	−0.010 (3)	0.000 (3)	−0.016 (3)
C17A	0.044 (3)	0.071 (4)	0.056 (4)	−0.007 (3)	0.007 (3)	−0.024 (3)
C18	0.084 (5)	0.074 (5)	0.056 (4)	−0.016 (4)	−0.003 (4)	−0.011 (4)
C18A	0.078 (4)	0.055 (4)	0.050 (3)	−0.025 (3)	0.008 (3)	−0.012 (3)

Geometric parameters (Å, º)

O1—C8A	1.382 (6)	C11—H11	0.9500
O1—C2	1.391 (6)	C11A—C12A	1.393 (7)
O2—C2	1.207 (6)	C11A—H11A	0.9500
O3—C4	1.260 (6)	C12—C13	1.391 (7)
O4—N2	1.416 (5)	C12—H12	0.9500

O4—H4O	0.94 (7)	C12A—C13	1.387 (7)
N1—C9	1.330 (7)	C12A—H12A	0.9500
N1—C10	1.428 (7)	C13—C14	1.487 (7)
N1—H1N	0.87 (6)	C14—C15	1.497 (7)
N2—C14	1.287 (6)	C15—H15A	0.9800
N3—C7	1.371 (6)	C15—H15B	0.9800
N3—C16	1.446 (7)	C15—H15C	0.9800
N3—C16A	1.453 (7)	C16—C17	1.533 (8)
C2—C3	1.441 (7)	C16—H16A	0.9900
C3—C9	1.396 (7)	C16—H16B	0.9900
C3—C4	1.425 (7)	C16A—C17A	1.521 (7)
C4—C4A	1.455 (7)	C16A—H16C	0.9900
C4A—C5	1.383 (7)	C16A—H16D	0.9900
C4A—C8A	1.385 (7)	C17—C18	1.510 (8)
C5—C6	1.378 (7)	C17—H17A	0.9900
C5—H5	0.9500	C17—H17B	0.9900
C6—C7	1.432 (7)	C17A—C18A	1.517 (8)
C6—H6	0.9500	C17A—H17C	0.9900
C7—C8	1.399 (7)	C17A—H17D	0.9900
C8—C8A	1.380 (7)	C18—H18A	0.9800
C8—H8	0.9500	C18—H18B	0.9800
C9—H9	0.9500	C18—H18C	0.9800
C10—C11	1.371 (7)	C18A—H18D	0.9800
C10—C11A	1.379 (7)	C18A—H18E	0.9800
C11—C12	1.394 (7)	C18A—H18F	0.9800

C8A—O1—C2	121.3 (4)	C13—C12A—C11A	120.7 (5)
N2—O4—H4O	103 (4)	C13—C12A—H12A	119.7
C9—N1—C10	127.6 (5)	C11A—C12A—H12A	119.7
C9—N1—H1N	110 (4)	C12A—C13—C12	118.3 (5)
C10—N1—H1N	123 (4)	C12A—C13—C14	120.4 (5)
C14—N2—O4	111.6 (4)	C12—C13—C14	121.2 (5)
C7—N3—C16	121.9 (5)	N2—C14—C13	115.5 (5)
C7—N3—C16A	120.2 (5)	N2—C14—C15	124.4 (5)
C16—N3—C16A	117.7 (4)	C13—C14—C15	119.9 (5)
O2—C2—O1	115.1 (5)	C14—C15—H15A	109.5
O2—C2—C3	127.5 (5)	C14—C15—H15B	109.5
O1—C2—C3	117.4 (5)	H15A—C15—H15B	109.5
C9—C3—C4	122.4 (5)	C14—C15—H15C	109.5
C9—C3—C2	115.1 (5)	H15A—C15—H15C	109.5
C4—C3—C2	122.5 (5)	H15B—C15—H15C	109.5
O3—C4—C3	122.6 (5)	N3—C16—C17	113.7 (5)
O3—C4—C4A	120.9 (5)	N3—C16—H16A	108.8
C3—C4—C4A	116.6 (5)	C17—C16—H16A	108.8
C5—C4A—C8A	117.2 (5)	N3—C16—H16B	108.8
C5—C4A—C4	123.3 (5)	C17—C16—H16B	108.8
C8A—C4A—C4	119.5 (5)	H16A—C16—H16B	107.7
C6—C5—C4A	122.1 (5)	N3—C16A—C17A	115.5 (5)
C6—C5—H5	118.9	N3—C16A—H16C	108.4
C4A—C5—H5	118.9	C17A—C16A—H16C	108.4
C5—C6—C7	120.3 (5)	N3—C16A—H16D	108.4
C5—C6—H6	119.9	C17A—C16A—H16D	108.4

C7—C6—H6	119.9	H16C—C16A—H16D	107.5
N3—C7—C8	121.8 (5)	C18—C17—C16	112.6 (5)
N3—C7—C6	121.0 (5)	C18—C17—H17A	109.1
C8—C7—C6	117.2 (5)	C16—C17—H17A	109.1
C8A—C8—C7	120.3 (5)	C18—C17—H17B	109.1
C8A—C8—H8	119.9	C16—C17—H17B	109.1
C7—C8—H8	119.9	H17A—C17—H17B	107.8
C8—C8A—O1	114.5 (5)	C18A—C17A—C16A	111.3 (5)
C8—C8A—C4A	122.8 (5)	C18A—C17A—H17C	109.4
O1—C8A—C4A	122.6 (5)	C16A—C17A—H17C	109.4
N1—C9—C3	121.8 (6)	C18A—C17A—H17D	109.4
N1—C9—H9	119.1	C16A—C17A—H17D	109.4
C3—C9—H9	119.1	H17C—C17A—H17D	108.0
C11—C10—C11A	121.3 (5)	C17—C18—H18A	109.5
C11—C10—N1	123.4 (5)	C17—C18—H18B	109.5
C11A—C10—N1	115.2 (5)	H18A—C18—H18B	109.5
C10—C11—C12	118.8 (6)	C17—C18—H18C	109.5
C10—C11—H11	120.6	H18A—C18—H18C	109.5
C12—C11—H11	120.6	H18B—C18—H18C	109.5
C10—C11A—C12A	119.5 (5)	C17A—C18A—H18D	109.5
C10—C11A—H11A	120.3	C17A—C18A—H18E	109.5
C12A—C11A—H11A	120.3	H18D—C18A—H18E	109.5
C13—C12—C11	121.4 (5)	C17A—C18A—H18F	109.5
C13—C12—H12	119.3	H18D—C18A—H18F	109.5
C11—C12—H12	119.3	H18E—C18A—H18F	109.5

C8A—O1—C2—O2	−177.4 (4)	C4—C4A—C8A—C8	179.5 (5)
C8A—O1—C2—C3	2.2 (7)	C5—C4A—C8A—O1	178.4 (5)
O2—C2—C3—C9	−2.3 (8)	C4—C4A—C8A—O1	−2.2 (8)
O1—C2—C3—C9	178.2 (4)	C10—N1—C9—C3	178.4 (5)
O2—C2—C3—C4	175.3 (5)	C4—C3—C9—N1	0.8 (8)
O1—C2—C3—C4	−4.2 (7)	C2—C3—C9—N1	178.4 (5)
C9—C3—C4—O3	−0.4 (8)	C9—N1—C10—C11	3.4 (8)
C2—C3—C4—O3	−177.9 (5)	C9—N1—C10—C11A	−177.9 (5)
C9—C3—C4—C4A	−179.6 (5)	C11A—C10—C11—C12	−0.3 (8)
C2—C3—C4—C4A	3.0 (7)	N1—C10—C11—C12	178.4 (5)
O3—C4—C4A—C5	0.5 (8)	C11—C10—C11A—C12A	−0.8 (8)
C3—C4—C4A—C5	179.6 (5)	N1—C10—C11A—C12A	−179.6 (5)
O3—C4—C4A—C8A	−179.0 (5)	C10—C11—C12—C13	0.3 (8)
C3—C4—C4A—C8A	0.2 (7)	C10—C11A—C12A—C13	2.1 (8)
C8A—C4A—C5—C6	−0.7 (8)	C11A—C12A—C13—C12	−2.1 (8)
C4—C4A—C5—C6	179.9 (5)	C11A—C12A—C13—C14	176.7 (5)
C4A—C5—C6—C7	1.4 (8)	C11—C12—C13—C12A	0.9 (8)
C16—N3—C7—C8	−170.1 (5)	C11—C12—C13—C14	−177.9 (5)
C16A—N3—C7—C8	4.2 (7)	O4—N2—C14—C13	−179.5 (4)
C16—N3—C7—C6	10.8 (8)	O4—N2—C14—C15	−4.5 (7)
C16A—N3—C7—C6	−174.9 (5)	C12A—C13—C14—N2	−20.3 (7)
C5—C6—C7—N3	177.6 (5)	C12—C13—C14—N2	158.5 (5)
C5—C6—C7—C8	−1.5 (8)	C12A—C13—C14—C15	164.4 (5)
N3—C7—C8—C8A	−178.2 (5)	C12—C13—C14—C15	−16.8 (8)
C6—C7—C8—C8A	0.9 (8)	C7—N3—C16—C17	75.6 (7)
C7—C8—C8A—O1	−178.7 (5)	C16A—N3—C16—C17	−98.8 (6)

C7—C8—C8A—C4A	−0.2 (8)	C7—N3—C16A—C17A	−83.8 (6)
C2—O1—C8A—C8	179.4 (4)	C16—N3—C16A—C17A	90.7 (6)
C2—O1—C8A—C4A	1.0 (7)	N3—C16—C17—C18	177.5 (5)
C5—C4A—C8A—C8	0.1 (8)	N3—C16A—C17A—C18A	−179.8 (5)

Hydrogen-bond geometry (Å, º)

D—H···*A*	*D*—H	H···*A*	*D*···*A*	*D*—H···*A*
O4—H4*O*···O3^{i}	0.94 (7)	1.80 (7)	2.707 (5)	160 (6)
N1—H1*N*···O3	0.87 (6)	1.87 (6)	2.626 (5)	145 (6)

Symmetry code: (i) −*x*+2, −*y*, −*z*+1.

11. REFERENCES:

1. Sheldrick, G. M., A short history of SHELX. *Acta Crystallogr., Sect A* **2008,** *64*, 112.
2. Sheldrick, G. M., Crystal structure refinement with SHELXL. *Acta Crystallogr., Sect C* **2015,** *71*, 3-8.
3. Barbour, L. J., X-Seed—A software tool for supramolecular crystallography. *J. Supramol. Chem.* **2001,** *1*, 189-191.
4. Ge, J.-F.; Arai, C.; Kaiser, M.; Wittlin, S.; Brun, R.; Ihara, M., Synthesis and in vitro antiprotozoal activities of water-soluble, inexpensive 3, 7-bis (dialkylamino) phenoxazin-5-ium derivatives. *J. Med. Chem.* **2008,** *51* (12), 3654-3658.
5. Davis, A. B.; Lambert, R. E.; Fronczek, F. R.; Cragg, P. J.; Wallace, K. J., An activated coumarin-enamine Michael acceptor for CN^-. *New J. Chem.* **2014,** *38* (10), 4678-4683.
6. Wallace, K. J.; Fagbemi, R. I.; Folmer-Andersen, F. J.; Morey, J.; Lynth, V. M. a.; Anslyn, E. V., Detection of chemical warfare simulants by phosphorylation of a coumarin oximate. *Chem. Commun.* **2006**, 3886-3888.
7. Mia, R.; Cragg, P. J.; Wallace, K. J., Low Molecular Weight Fluorescent Probes for the detection of organophosphates. *J. Lumin.* **2021,** *235*, 118053.
8. *Spartan '20* (v 1.1.1), Wavefunction Inc., 18401 Von Karman Ave., Suite 435, Irvine, CA 92612, USA